Article

Evaluation of Terbutaline Adsorption from Aqueous Medium by Mechanically Generated [Cu (INA)$_2$]-MOF Metal-Organic Framework and its Modified Magnetic Composite ([Cu (INA)$_2$]-MOF@Fe_3O_4)

Usman Armaya'u [1,2], Marinah Mohd Ariffin [1*], Saw Hong Loh [1], Wan Mohd Afiq Wan Mohd Khalik [1], Hanis Mohd Yusoff [1]

[1] *Faculty of Science and Marine Environment, Universiti Malaysia Terengganu, Malaysia.*; p4222@pps.umt.edu.my (U.A.); ohsh@umt.edu.my (S.H.L.); wan.afiq@umt.edu.my (W.M.A.); hanismy@umt.edu.my (H.M.Y.)
[2] *Faculty of Applied Sciences, Al-Qalam University Katsina, Nigeria*
* Correspondence: **erin@umt.edu.my (M.M.A)**

Abstract: Mechanochemical production of copper (II) isonicotinate Metal-Organic Framework ([Cu (INA)$_2$]-MOF) and its modified magnetic iron composite ([Cu (INA)$_2$]-MOF@Fe_3O_4]) allowed for the adsorptive removal of Terbutaline from water. A variety of characterization techniques, including Fourier, transform infrared spectroscopy (FTIR), thermogravimetric analysis (TGA), X-ray diffraction (XRD), and scanning electron microscopy (SEM), were used to elucidate the distinct chemical and morphological features of the two advanced materials. The optimal adsorption conditions were determined by investigating a wide range of adsorption-related variables, including contact time, initial Terbutaline concentration, adsorbent dosages pH, and temperature. The chemistry involved in the adsorption process between the adsorbents and the adsorbate molecules was evaluated using the best-fitting models, such as kinetics, isotherms, and thermodynamics, and the regeneration study was performed to evaluate the adsorbents' reusability. Incredibly maximum adsorption capacities (Q_{max}) of 1667 and 2500 mg L^{-1} were attained within 40 minutes under alkaline pH 11 by the [Cu (INA)$_2$]-MOF and the [Cu (INA)$_2$]-MOF@Fe_3O_4, respectively. The adsorbents have been proven to be good for the adsorption of Terbutaline as a priority pollutant in an aqueous solution, with pseudo-first order and Langmuir as the best-fitting models for the kinetic and isotherm models respectively.

Keywords: Adsorption; β-agonists; Magnetic-composite; Metal-Organic Frameworks; Pollutant; Removal; Terbutaline

1. Introduction

The contamination of the natural world has quickly assumed the position as one of the most critical challenges now confronting human civilization [1]. Water bodies are continuing to deteriorate as a direct result of the decrease in water quality, which has led to the suspension of significant factory operations that differ in a variety of ways, including human activities as well as the production of agricultural goods. These halted factory operations have had a variety of effects, including on human activities as well as agricultural production. The negative social effect and economic loss caused by the event represent a threat to the continuing healthy growth of humanity as well as to society's ability to develop in a sustainable manner [2]. Indicative data for the presence of drugs in an environment was first released by Hignite between 1977 and 1978 [3]. While recent reports trigger the attention of policymakers and scientists all around the globe that the distribution, use, and manufacture of pharmaceuticals and other related substances are substantial

 doi:10.20944/preprints202212.0434.v1

contributors to the contamination of the world's water supplies by organic pollutants [4]. While the very recent reports on environmental contamination have shifted attention to initiatives aimed at reducing and remediating the contamination [5]. Pharmaceuticals are developed and used to serve several purposes including fighting, reducing, eliminating, detecting, and treating illness, preventing its recurrence, and restoring or changing normal bodily processes. β-agonists are man-made substances that are developed in the pharmaceutical industry to achieve the desired effects of muscle relaxation and airway dilation to facilitate easier breathing. They are catecholamine derivatives that generate physiological effects such as an irregular heartbeat by binding to β-receptors on nerve cells, also known as β-adrenoceptors [6]. Their mode of action is analogous to that of epinephrine, norepinephrine, and dopamine, which triggered nerve endings in the bloodstream to induce autonomic or involuntary action of the nervous system (mostly experienced terbutaline potential implication), as Terbutaline was found to trigger nerve endings in the bloodstream to induce autonomic or involuntary action of the nervous system [7]. Asthma [8], chronic obstructive pulmonary disorders (COPD) [9], cough suppressants [10], bradyarrhythmia (an abnormally fast heartbeat) [11], and tocolytic therapy [12] are some of the conditions that β-agonists are commonly used to treat. Medical studies have also revealed that β-agonists not only alleviate asthma symptoms, but also boost muscle protein, decrease overall body fat by causing the breakdown of stored fat, enhance muscle growth in people and animals, and increase the efficiency with which feed is converted into muscle [13]. Even though -agonists can be used as medicine, many people with severe asthma attacks have been found to self-medicate and use too many of them. Athletes have used them to boost lipid metabolism and build muscle. They have also been used illegally in livestock feed to make animals grow faster and make learner meat. So, food, agriculture, medical, and sports agencies at both the national and international levels have passed laws and rules about the use of some β-agonists because people use them without a doctor's permission or on their own [14]. With the official concentration on detection slated as 0.5 g m L^{-1} using GC–MS after derivatization, this puts the concentration exceeding 1 g m L^{-1} as a doping violation range. Athletes are prohibited from using it either orally or parenterally, according to the Medical Commission of the International Olympic Committee and the World Anti-Doping Agency (WADA) [15]. Terbutaline ($C_{12}H_{19}NO_3$) is a 5-[2-(tert-butyl amino)-1-hydroxyethyl] benzene-1, 3-diol molecule [16], as shown structurally in Figure 1 is a β-agonist with a water solubility of 5.84 mg/mL, a molecular weight of 225 g/mol, and a pK_a of 9.12 [17] [18]. It is commonly used as a bronchodilator to increase lung airflow and as a tocolytic to slow uterine contractions and reduce preterm delivery [19]. Terbutaline can also be used to treat other bronchospasms symptoms like chest tightness, difficulty breathing, and wheezing. Reports on the abuse of Terbutaline have been given from overdoses in patients with respiratory disorders [20] to some recent cases of β-agonist toxicity among young athletes by [21]. Due to their direct effect on metabolic processes, these chemicals are extremely toxic to organisms. For instance, β-agonists may alter testosterone levels and reduce fecundity[22]; more research indicates that a higher dose of terbutaline stimulates β-receptors, posing a threat to human health, including tachycardia, nervousness, muscle tremors, fatigue confusion, headache, dizziness, chest distress, heart palpitations, anxiety, insomnia, itching, and limb numb [5]. Its off-label usage for the long-term treatment of preterm labour is associated with an increase in neurodevelopmental abnormalities, including autism spectrum disorders. It is often administered through inhalation, oral, or injectable [23].

This research uses terbutaline as a model analyte due to its detrimental environmental effects and toxicity to people and aquatic species because of its persistent entrance into the ecosystem.

Preprints (www.preprints.org) | NOT PEER-REVIEWED | Posted: 23 December 2022 doi:10.20944/preprints202212.0434.v1

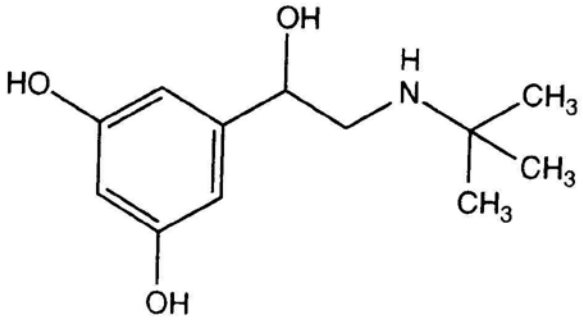

Figure 1. Terbutaline Model

Approximately 70% of the volume of medicines taken by people or animals is excreted as a combination of non-metabolized medications without any change in their chemical structure and conjugated metabolites, according to studies [24]. Thus, the unchanged parent components of the unmetabolized excreted substances are released into sewage treatment facilities or our ambient waterways. Possible health impacts from long-term exposure to pharmaceutical β-agonists through drinking water have been well hypothesized [5], and subsequent studies determined their effects on living species as hazardous to aquatic life and people [20] [25]. Higher concentrations of β-agonist in fish plasma are linked to human pharmacological effects [26]. While frequent reports of their occurrences in our environmental waters raises more concerns [27] [5]. Pharmaceutical industries, hospitals, poultry farms, and slaughterhouses as well as personal use in our individual houses releases them into the environment, and their presence is widespread in home tap water [28]. Due to their toxicity, it's important to develop a simple and efficient strategy to remove these compounds from environmental waterways, as the old method does not remove them completely.

Previous literature reported that β-agonists can be removed through oxidation [29], photo-degradation [30], and adsorption [17], but, since oxidation and photocatalytic degradation produce harmful intermediates, adsorption is always chosen as the most attractive, simple, promising, affordable, and friendly method for removing contaminants during wastewater recovery [31]. Therefore, scientists continued their quest for the novel adsorbents with the very good properties in adsorption studies. The reported adsorbents for β-agonists removal were Molecularly Imprinted Polymers [32] [33], anionic cellulose nanofibrils [34], Micro-grain activated carbon (μ-GAC) [31], and granular activated carbon (GAC) [35]. But most of these adsorbents have limited adsorption effectiveness with extended equilibrium times, and problematic and difficulty in regeneration. Thus, the quest for more natural and manmade porous materials are still considered necessary for the effective removal β-agonists.

Metal-organic frameworks (MOFs) are a type of microporous material that has just been found for use in environmental remediation. The framework of the MOF is highly crystalline, with large surface areas, a flexible number of pores and cavities, and chemical stability, allowing for superior performance and a larger range of applications as adsorbents than traditional materials [36]. The outstanding adaptability and practical uses of MOFs that differ from other traditional porous solids as well as simple and easy synthesis have been some of the many intriguing ways that researchers in academia and industry have been drawn to them [37]. The potentials of MOF materials to be utilized in molecular separations and selective adsorption is observed by Janiak [38]. And their selective adsorption patterns in comparison to shape, size, hydrophobic and hydrophilic features are fascinating to examine, and they pave the way for practical applications, most notably in gas molecule separation, which is now under research [39]. Based on the interpenetration

 doi:10.20944/preprints202212.0434.v1

network structures packed by hydrogen bonding and pi stacking, it is expected that the selective adsorption profiles of MOF based on shape, size, hydrophobic and hydrophilic properties will be promising for the selective adsorption of persistent pollutants such as terbutaline, based on the interpenetration network structures packed by hydrogen bonding and pi stacking. Weaker noncovalent interactions, such as hydrogen bonding or pi-pi stacking, are essential for chain packing in one, two, and three-dimensional frameworks.

Due to their versatility, they are of great interest in both scientific and technological fields, such as liquid adsorption [40], catalysis [41], sensing [42], electrochemistry and conversions [43] as well as in biological applications such as the drug deliveries and contrasting agents [44]. A re-evaluation of the literature on the removal of β-agonists in environmental waters indicated that few research were conducted using the newly discovered materials (MOFs). In 2019, Yang [42] synthesized and utilized fluorescent zirconium-based MOF (Ui0-66) by hydrothermal synthesis for the determination and removal of β-agonist in water, the removal of terbutaline using chromium based thin-film Nanocomposite MOF in 2020 by Ruobin Dai [45] and in 2021, through the utilization of aluminum-based MOF (BUT-19) by solvothermal synthesis for the removal of β-agonists by Lv [46]. Both synthesis processes were on some disadvantages, as they took hours to days using toxic solvents. But synthesis of functionalized materials using a green chemistry approach eliminates or reduces the generation of hazardous waste that is harmful to human health and the environment.

Now, the adjustable cavities and tailorable chemical compositions of the MOFs enable the development of materials with specific properties. As an illustration, Zeng [47] developed novel molecular magnetic alloy materials that include mixed metal ions and chiral dicarboxylates into a crystalline MOF material to form a solid structure with adjustable cavities and customizable chemical compositions. For the ease with which MOFs can be manipulated, their potential is constantly expanding, resulting in a greater number of research articles showcasing MOFs as an important category of materials. Among these adaptations is the fabrication of composite-MOFs, (Multi-component materials are referred to as composites), which comes up with multiple discrete phases as well as at least one continuous phase.

Due to their adaptability, MOFs composites, which are frequently used in adsorption, have recently been receiving a lot of attention. Numerous studies have covered the synthesis of MOFs-composites and its intriguing applications. MOF compositions may benefit from the addition of functionalized components in terms of their synthesis rates, form, physicochemical characteristics, stability, and even possible applications. By introducing active groups or impregnating the right active materials, modifying organics, and developing composites with the right specifications, we may enhance the physiochemistry of materials [48]. Selectivity is one of the most fundamental issues that should be addressed by an appropriate adsorbent in the real application. It is possible to customise MOF-based adsorbents with a range of functional groups to remove certain pollutants. This will allow for the ability to solve the issue. These components can be easily integrated for adequate selectivity using magnetic-MOF composites.

The targeted integration of magnetic nanoparticles (MNPs) and MOFs is leading to the development of new multifunctional MOF-based composites with better performance than either the MNPs or MOF alone [2]. It was also possible to create MOFs with magnetic properties by incorporating nanomaterials into the framework of the MOF. The magnetic composite metal-organic frameworks (MCMF) are formed when MNPs are coupled with MOF. Enough vacant sites in these MFCs make it possible to selectively separate the desired compounds, and they also have the all-important magnetic separation ability. In 2018 [49] used a mechanochemical process to design a new magnetic porous MOF-nanocomposite by using the ball milling grinding method, and the resulting material had a

 doi:10.20944/preprints202212.0434.v1

good porosity and a good magnetic ability with good adsorption capacity. All these possibilities, as well as a slew of others, were made possible due to the tailorable chemistry of MOF and the composites in tunable cavities.

While in the field of water purification, nano-magnetic structured adsorbents perform better than traditional materials due to their greater efficiency and quicker adsorption rates, both of which are a result of their larger surface area as well as their magnetic ability. In solutions, the functionalization of the iron oxide hydroxyl occurs as a result of the formation of a covalent bond between the Fe atoms and the water molecules. Complexes are formed between the atoms of the iron oxide and molecules on the surface of the iron oxide that are rich in lone-pair electrons. As a result of their amphoteric nature, the oxygen groups in question can react with both acids and bases.

Much successful research has been aided by the combination of the 3D network's strong magnetic intercluster interaction with the secondary building units (SBU's) inherent properties. Adding the second type of metal ion to the crystal lattice in a MOF with only one type of metal ion has been demonstrated to be both technically feasible and theoretically feasible [47], resulting in a solid product that could be used to control the number or uniformity of SBU linkages between metal centres, resulting in an increased and controlled ordering of mixed-metal ions in a polycrystalline MOFs that could show rich properties.

Along with chemisorption and/or physisorption, the physical and chemical properties of magnetic nanoparticles (such as particle size, surface area, surface charge, accumulation/aggregation, shape, and surface coating) can be utilised to adsorb β-agonists from contaminated water. Our decision to employ iron oxide nanoparticles was inspired by the relative benefits and practical applications of nanomaterials, which led us to select iron oxide nanoparticles (Fe_3O_4-MNPs) as our material of choice. Some proven researches has been discovered that Fe_3O_4 nanoparticles have a high conductivity, a wide surface area, and a good adsorptive ability towards amine and other non-amine compounds [49] [50] [51].

To remove β-agonists from water, we proposed and redesigned metal-organic framework composited with magnetic nanoparticles as more permeable conventional and synthetic materials. MCMF research are extremely recent and their applications in water remediation, in general, are very rare and no MCMF studies on β-agonists have been documented. Both the Mechanosynthesis and study using metal-organic frameworks (MOFs) and the MCMFs on Terbutaline adsorption from water has not been done so far, based on the author's findings. Numerous techniques, including coprecipitation, sol-gel, hydrothermal, electrochemical, and micro emulsion synthesis, have been developed in order to facilitate the production of Fe_3O_4 nanoparticles [52]. For the manufacture of Fe_3O_4 nanoparticles, the mechanosynthetic approach is by far the most prepared option since it is both straightforward, environmentally friendly and very effective too [49].

According to the reviewed literature, various studies have used MOF composites in the same way as their virgin MOFs to purify water, and the composites were shown to have greater removal rates and adsorption capacities than the virgin MOFs. Methylene blue (MB) was successfully removed from samples by utilising GO/HKUST 1 composites, according to Li's study [53]. While the adsorption capacity of pure HKUST-1 for removing MB was only about half, the adsorption capacity of the GO/HKUST-1 composite was as much as eight times that of the MOF alone. Anbia [54], also synthesised an acid-treated MWCNT@MIL-101 MOF hybrid composite with superior adsorption capacity, almost 60% higher than that of non-modified MOF. Consequently, similar evidence supported Ahmed's claim [55], that MOF may be utilised as a prepared adsorbent because of their versatility and the ease with which they can be changed brought about by recent

Preprints (www.preprints.org) | NOT PEER-REVIEWED | Posted: 23 December 2022 doi:10.20944/preprints202212.0434.v1

developments in the composite and functionalization of MOF. Zakariyya [56] rigorously investigated adsorption employing MOFs and their composites, and after seeing their outstanding findings, he labelled the composite-MOFs as super adsorbents since they provide more selectivity to organic pollutants.

A new iron oxide MNPs copper (II) isonicotinate-based MCMF ([Cu (INA)$_2$]-MOF@Fe_3O_4) that has a Cu (II) square-pyramidal geometry with extremely high chemical lability and hydrophobicity using a mortar and pestle was prepared in our Laboratory, with the aim of improving the adsorption of Terbutaline in our environmental waters by optimizing the various parameters. An adsorption study was performed with the non-modified [Cu (INA)$_2$]-MOF and the new synthesized magnetic [Cu (INA)$_2$]-MOF@Fe_3O_4 manufactured in our lab and the two were used in this work with great success. The both [Cu (INA)$_2$]-MOF and [Cu (INA)$_2$]-MOF@Fe_3O_4 have particular capabilities that aid in selectively adsorbing Terbutaline, with special functionalities.

Production of functionalized materials via a green chemistry method eradicates or decreases the generation of dangerous perilous waste that is destructive to human health and the environment, at the same time removing environmental contaminants like β-agonists that are micro and non-volatile found in our environmental waters. It was decided to make and employ copper in a copper-based MOF due to copper's known non-toxic effects, the biocompatibility of the composite components, and their properties that were efficient for the final application. As an adsorbent for the novel hazardous removal material of β-agonist compounds in aqueous solution, the successful and ecologically acceptable (green) approach of combining mortar and pestle grinding and heating of solid reactants is presented here. As an adsorbent, the resultant microporous and stable Cu-based MOF [Cu (INA)$_2$]-MOF and its modified [Cu (INA)$_2$]-MOF@Fe_3O_4 are employed here. The present ([Cu (INA)$_2$]-MOF and the [Cu (INA)$_2$]-MOF@Fe_3O_4 are determined to fulfil the MOF and composite-MOFs benchmarks, which include outstanding thermal and chemical stability, adequate porosity, avoiding substantial impurities, and sustainability [57].

We opt for the solvent-free synthesis (Mechanosynthesis) method for its many advantages over Solvosynthesis (synthesis using solvents) method which includes no toxic and hazardous solvent, shorter reaction time, money-saving, environmentally friendly chemicals, quick and easier synthesis as well as obtaining higher/quantitative yield.

2. Materials and Methods

2.1 Chemicals and materials

All the chemicals used in this work were analytically graded and used as received. Copper acetate monohydrate (98.5%), isonicotinic acid (98%), Terbutaline sulfate, ferrous chloride heptahydrate, and ferric chloride hexahydrate were purchased from Sigma Aldrich (St. Louis, MO, USA). methanol (99.5 %), sodium hydroxide, and hydrochloric acid were supplied by IT Tech Research Selangor, Malaysia.

2.2 Synthesis of isonicotinate Metal-organic Frameworks [Cu (INA)$_2$]-MOF

[Cu (INA)$_2$]-MOF was synthesized by a solvent-free technique following the procedure reported by Tella (A. Tella et al., 2016) with little modification. Briefly stated, 0.25 g (1mmol) of copper acetate monohydrate (Cu $(CH_3COO)_2H_2O$) and 0.246 g (2mmol) isonicotinic acid ($C_5H_4N(CO_2H)$ were mixed and grounded together for 10 minutes using mortar and pestle. The formation of the product was followed by a characteristic odour of acetate and the evidence of the colour change from green to blue. The product obtained

Preprints (www.preprints.org) | NOT PEER-REVIEWED | Posted: 23 December 2022 doi:10.20944/preprints202212.0434.v1

was then heated at 150°c for 12 hours to remove the glacial acetic acid trapped in the pores of the [Cu (INA)$_2$]-MOF. The product was kept in a desiccator to cool after which the sample was stored in the sample bottle and later used without any additional treatment during the experimental work.

2.3 Mechano-synthesis of Fe_3O_4-MNPs

Fe_3O_4-MNPs was made utilizing an innovative mechanochemical method that was similar to the one previously reported by Bellusci [49] with only slight changes. In a typical procedure, 5 g of a molar ratio combination of reactants $FeCl_36H_2O$, $FeCl_24H_2O$, and NaOH, were thoroughly mixed in a mortar and pestle. To reduce the formation of crystalline development phenomena, NaCl was added in excess (to the tune of 100 wt %) to the stoichiometric mixture as a phase control agent. The synthesis was accomplished by crushing the components continuously in a mortar and pestle. The materials combination was collected after 30 minutes of grinding, and the powder was washed with water before being dried at 70°C under a vacuum and kept until future use.

The complete equation for the reaction of the Fe_3O_4-MNPs synthesis using Mechano-synthesis method is given below from Jannah [52].

$$Fe^{2+} + 2OH \rightarrow Fe(OH)_{2(s)} \quad (1)$$

$$Fe^{3+} + 3OH \rightarrow Fe(OH)_{3(s)} \quad (2)$$

$$Fe(OH)_{2(s)} + Fe(OH)_{3(s)} \rightarrow Fe_3O_{4(s)} + 4H_2O \quad (3)$$

2.4 Mechano-synthesis of magnetic composite metal-organic framework (MCM) [Cu (INA)$_2$]-MOF@Fe_3O_4

For the [Cu (INA)$_2$]-MOF@Fe_3O_4 synthesis, the Bellusci (Bellusci et al., 2012) (Bellusci et al., 2018) approach was modified; briefly, Fe_3O_4-MNPs was first functionalized with the [Cu (INA)$_2$]-MOF by neat grinding in a mortar with a pestle. At the outset, 0.5 g of Fe_3O_4-MNPs and 0.43 g of [Cu (INA)$_2$]-MOF were appropriately weighed into the mortar. The mixture was grinded together for 10 minutes, 0.2 g of $FeCl_36H_2O$. The samples were purified using ethanol and water. To summarise, tidy grinding was used to successfully functionalize the Fe_3O_4-MNPs with the [Cu (INA)$_2$]-MOF making the magnetic composite copper (II) isonicotinate metal-organic framework [Cu (INA)$_2$]-MOF@Fe_3O_4.

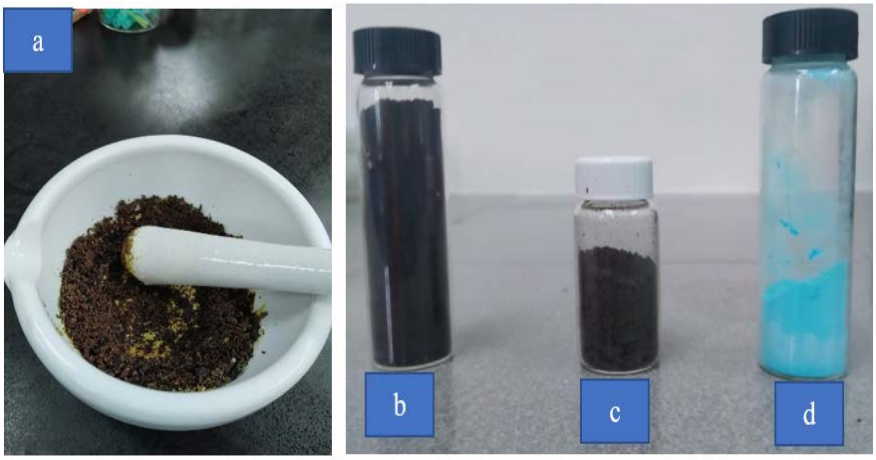

Figure 2. a) Synthesis process of Fe_3O_4-MNPs b) Synthesized Fe_3O_4-MNPs c) Synthesized [Cu (INA)$_2$]-MOF@Fe_3O_4 c) Synthesized [Cu (INA)$_2$]-MOF.

 doi:10.20944/preprints202212.0434.v1

2.5 Characterization

For the Fourier transformed infrared spectroscopy (FTIR) PerkinElmer FTIR spectrometer was used to characterize the MOF for functional groups in the 400 to 200 cm^{-1} spectral region. A thermogravimetric analyzer (Shimadzu TGA-50 Analyzer) was used to test thermal stability by heating the material at 10 °C/minute in an inert environment (Ar). The topography, microstructure, and elemental evidence were determined using scanning electron microscopy (SEM) Zeiss Supra 55 VP instrument). Finally, powdered X-ray diffraction (XRD) was performed to determine crystallinity using Bruker D8 Advance X-ray Diffractometer The 4-50° 2 range data was taken with a 0.02° step width.

2.6 Removal Experiment

2.6.1 Preparation of Terbutaline solutions

To make a stock solution of terbutaline (100 mg L^{-1}) in methanol, 1 mg was dissolved in a 100 mL volumetric flask. The produced solution was stored at 4 °C in the refrigerator. Every day, right before the adsorption experiments, the working solutions were made with milli-Q water by diluting the stock solution to get the required amount. As methanol is miscible with water, it is possible to separate polar components from non-polar components by mixing Methanol and water. The advantages of using a mixture of methanol and water include lowering the surface tension, decreasing the polarity of the water, increasing the density, and possibly allowing specific compounds to collect at the interface.

2.6.2 Batch adsorption study

After diluting the stock solution with milli-Q water to make the working solution, adsorptions at various concentrations were conducted. [Cu $(INA)_2$]-MOF and [Cu $(INA)_2$]-MOF@Fe_3O_4 were individually suspended in a 150 mL conical flask containing 10, 20, 30, 40, 50, and 60 mg L^{-1} initial concentrations of terbutaline solution. The flask was then placed inside a temperature-controlled incubator shaker (stacked shaker SKE 8000) and shaken at 150 rpm for approximately 120 minutes. About 2 mL aliquot of the sample solution was collected at 10 minutes intervals and using filter 0.45 m nylon syringe membrane The absorbance of terbutaline in the filtrate solution was measured at λ_{max} 283 nm by UV-Vis spectrophotometer (Shimadzu UV-1800) using a quartz cuvette. The impacts of pH were explored by varying the pH of the solution from 3, 5, 7, 9, 11, and 13 with 0.1 NaOH and M HCl before reaching the final volume of 40 ml, whilst the effects of temperature were investigated by varying the temperature from 25, 30, 35, 40, 45, and 50 °C. The adsorbent dose was also varied between 1, 2, 3, 4, 5, and 6 mg g^{-1}.

The percentage removal (%R), quantity adsorbed at a certain time interval (q_t) as well as the quantity adsorbed at equilibrium (q_e) were determined using equations 4, 5 and, 4 as presented by [58] [59] as follow;

$$\%\mathbf{R} = \frac{(C_0 - C_t)}{C_0} \boldsymbol{X}\ \mathbf{100} \tag{4}$$

$$\boldsymbol{q_t} = \frac{(C_0 - C_t)V}{W} \tag{5}$$

$$\boldsymbol{q_e} = \frac{(C_0 - C_e)V}{W} \tag{6}$$

Where C_0 (mg L^{-1}) is the initial concentration, C_t (mg L^{-1}) is the concentration at a time t (minutes), and C_e (mg L^{-1}) is the equilibrium concentration of terbutaline. W is the dried weight of the adsorbent (g), and V is the volume of the studied solution (L).

Preprints (www.preprints.org) | NOT PEER-REVIEWED | Posted: 23 December 2022 doi:10.20944/preprints202212.0434.v1

All the adsorption data were collected in triplicate, and the average values were determined from the data.

2.6.3 Regeneration study

The regeneration and reuse properties were evaluated for both [Cu (INA)$_2$]-MOF and [Cu (INA)$_2$]-MOF@Fe_3O_4. The [Cu (INA)$_2$]-MOF and [Cu (INA)$_2$]-MOF@Fe_3O_4 residue were washed with absolute methanol (50 mL) and then with distilled water before being vacuum dried for 3 hours at 100 °C and kept in the desiccator after the adsorption study. The regenerated adsorbents were also used for terbutaline adsorption for five consecutive cycles under optimum circumstances similar to the batch adsorption studies mentioned in section 2.6.2.

2.6.4 Adsorption isotherms

The equilibrium relationship between the adsorbate and the adsorbents that determines the relative affinity of each of the adsorbents (the [Cu (INA)$_2$]-MOF and the [Cu (INA)$_2$]-MOF@Fe_3O_4) to the terbutaline was described using isotherm modelling according to Langmuir, Freundlich, and Temkin as described by the linear equations (7), (8), and (9), respectively (Isiyaka, Jumbri, Sambudi, Zango, et al., 2021).

$$\frac{C_e}{q_e} = \frac{1}{K_L q_m} + \frac{1}{q_m} C_e \quad (7)$$

$$\log q_e = \log K_F + \frac{1}{n} \log C_e \quad (8)$$

$$q_e = \frac{RT}{b_T} \ln A_T + \left(\frac{RT}{b_T}\right) \ln C_e \quad (9)$$

Where q_m is the adsorption capacity, K_L is the Langmuir constant, K_F is the Freundlich constant, 1/n represents the adsorption intensity, b_T (kJ/mol) represents the Temkin constant which relates to the heat of adsorption, A_T is the equilibrium binding constant corresponding to the maximum binding energy. T is the absolute temperature, and R is the Universal gas constant.

Moreover, these models were fitted with statistical regression analysis to define the coefficient of determination (R^2), adjusted coefficient of determination (R^2 adj.), root means square error (RMSE), and Akaike information criterion (AIC) as criteria to assess the model performance, using the equations 10, 11 and 12 below [40]

$$R^2 = 1 - \frac{\Sigma(q_{e\,exp} - q_{e\,cal})^2}{\Sigma(q_{e\,exp})^2} \quad (10)$$

$$RMSE = \sqrt{\sum_{n=1}^{i} (q_{e\,exp} - q_{e\,model})^2} \quad (11)$$

$$AIC = n \ln\left(\frac{SSE}{n}\right) + 2n_p + \frac{2n_p(n_p+1)}{n(n_p+1)} \quad (12)$$

Where $q_{e\,exp}$ and $q_{e\,model}$ represents experimental and model adsorption capacity, n is the number of observations and p denotes the number of parameters. SSE is the sum of the square errors obtained. A higher R^2 value indicates better linearity of the models while smaller RMSE, AIC indicate better fitting of the model.

2.6.5 Kinetic study

Preprints (www.preprints.org) | NOT PEER-REVIEWED | Posted: 23 December 2022 doi:10.20944/preprints202212.0434.v1

The kinetics analysis gives a thorough mechanism for the adsorption process as well as the rate-controlling step. The kinetics model tells us how fast a solute move from an aqueous environment to a solid-phase interface at a certain dose of adsorbent, temperature, flow rate, and pH at a specific time rate. Thus, in this study, the data for terbutaline adsorption onto both the [Cu (INA)$_2$]-MOF and [Cu (INA)$_2$]-MOF@Fe_3O_4 were subjected to three major models, namely, pseudo-first-order, pseudo-second-order, and intra-particle diffusion, represented by equations (13), (14), and (15), respectively [40] [60].

$$\boldsymbol{ln(q_e - q_t) = ln\, q_e - k_1 t} \quad (13)$$

$$\frac{\boldsymbol{t}}{\boldsymbol{q_t}} = \frac{\boldsymbol{1}}{\boldsymbol{k_2 q_e^2}} + \frac{\boldsymbol{t}}{\boldsymbol{q_e}} \quad (14)$$

$$\boldsymbol{q_t = K_P t^{1/2} + C} \quad (15)$$

The values $\boldsymbol{q_e}$ and $\boldsymbol{q_t}$ are the amount of the terbutaline adsorbed at equilibrium and at a certain time respectively, k_1 and k_2 are the pseudo-first order and pseudo-second-order rate constants, respectively. K_P is the intraparticle diffusion rate constant and C is constant.

2.6.6 Thermodynamics study

The thermodynamics research provides information on the nature of the adsorption process based on temperature differences. Thermodynamic parameters such as Gibbs free energy change (ΔG°), standard enthalpy change (ΔH°), and entropy change (ΔS°) for the process were calculated using Van't Hoff equations (16), (17), and (18) based on the temperature dependence of the adsorption process [61].

$$\Delta G° = - RT\ln \boldsymbol{K_d} \quad (16)$$

$$\boldsymbol{K_d} = \frac{\boldsymbol{q_e}}{\boldsymbol{C_e}} \quad (17)$$

$$\Delta G° = \Delta H° - T\Delta S° \quad (18)$$

3. Results

3.1 Characterizations

Figures 2a, 2b and 2c show the infrared spectra of [Cu (INA)$_2$]-MOF and [Cu (INA)$_2$]-MOF@Fe_3O_4. The major peak at 3434 cm^{-1} was generated by OH stretching from the copper acetate and isonicotinic acid linker, which served as the MOF's secondary building units. A strong signal at 1602 cm^{-1} in the spectra revealed that the isonicotinic acid linker was deprotonated. The appearance of the peak at 1562 cm^{-1} was due to COO– asymmetric stretching, while the peak at 1503 cm^{-1} was due to COO–symmetric stretching due to the organic linker, respectively. The stretching vibration that emerged in the MOF at 1722 cm^{-1} indicates that the isonicotinic acid is completely coordinated [62]. The absorption band at around 776 cm^{-1} is the development of the Cu-O coordination bond [63]. Given that the pyridine ring's nitrogen contributes to the coordination sphere, the peak at 1382 cm^{-1} reveals the stretching in the C=N [62]. The Fe_3O_4-MNPs FTIR spectrum clearly reveals the distinctive peaks at 525.60 and 633.66 cm^{-1}, which correspond to the stretching vibration mode of Fe-O bonds, while the bending and stretching vibration modes of -OH groups present in the Fe_3O_4-MNPs peaks were found at 1629.87 and 3324 cm^{-1} [51] [64]. The magnetite phase in the Fe_3O_4-MNPs is validated by the absorption band located at 525.60 cm^{-1}. While the FTIR spectrum of the [Cu (INA)$_2$]-MOF@Fe_3O_4 also validated the Fe_3O_4-MNPs by the absorption band occurring around 536.39 cm^{-1}. The isonicotinate molecule appears to be in tune

Preprints (www.preprints.org) | NOT PEER-REVIEWED | Posted: 23 December 2022 doi:10.20944/preprints202212.0434.v1

with the stretching vibration at 1717 cm^{-1} in the [Cu(INA)$_2$]-MOF@Fe_3O_4 despite being stretched from a [Cu (INA)$_2$]-MOF [62]. It was observed that the band with a relative intensity spanning from 3434 to 3416 to 3324 cm^{-1} has a decline in all between the compounds formation, this discovery might be due to the creation of a complex on the adsorbent surface involving the cations Cu^{2+} and Fe^{3+}, as well as the isonicotinate's amine groups (copper Isonicotinate/Fe_3O_4 nanocomposite adsorbent) [65]. Moreover, a new band could be seen at 839 cm^{-1} (ring-out-of-plane vibrations of the substituted aromatic of the linker molecules). These results indicate that the coordination process was successful, with relatively few unreacted linker residues left. Due to overlap with other peaks, the presence of iron oxides in composite materials is not easily detectable by infrared (IR) analysis [49].

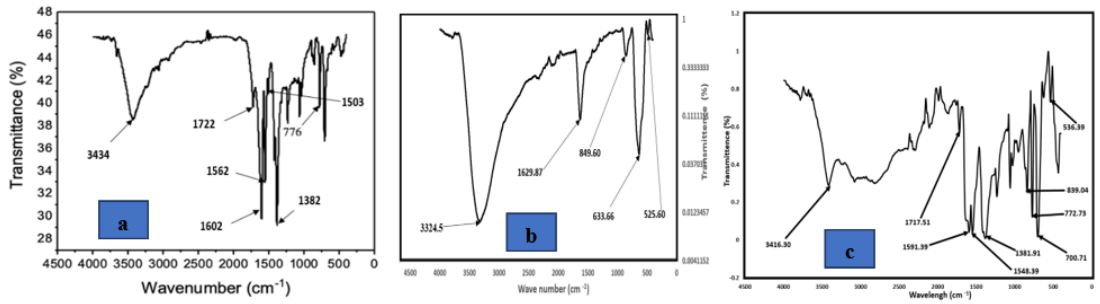

Figure 2. Spectra of the a) [Cu (INA)$_2$]-MOF b) Fe_3O_4-MNPs c) [Cu (INA)$_2$]-@Fe_3O_4)-MOF

Figures 3a, b, and c depict the TG thermograms of the [Cu (INA)$_2$]-MOF, the Fe_3O_4-MNPs, and the [Cu (INA)$_2$]-MOF@Fe_3O_4). Presenting the TGA curves as a function of % mass loss over temperature. The crystal [Cu (INA)$_2$]-MOF was subjected to TGA with an initial mass of 4,642 mg. heating from 100.00 °C to 900.00 °C, the complete TG analysis was performed at a heating rate of 10,00 °C/min. [Cu (INA)$_2$]-MOF complex was thermally stable up to 250 °C, with a significant weight loss of 82% at 246.38 °C and 322.66 °C [66], confirming the absence of a solvent molecule within the framework and revealed the material has excellent thermal stability.

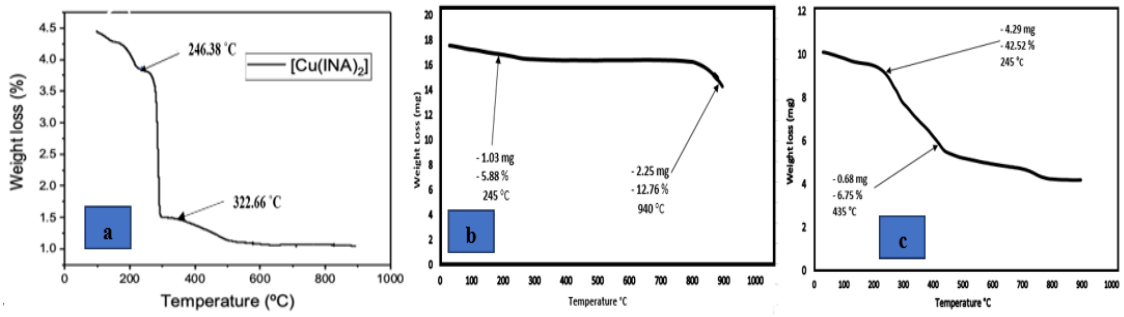

Figure 3. Thermograms of a) [Cu (INA)$_2$]-MOF b) Fe_3O_4-MNPs c) [Cu (INA)$_2$]-MOF@Fe_3O_4)

While in both the ([Cu (INA)$_2$]-MOF@Fe_3O_4) and Fe_3O_4-MNPs two main weight losses were demonstrated. The results of the thermogravimetric analysis of the Fe_3O_4 are displayed in Figure 3b and it demonstrates a slight weight loss of 5.8 (wt. %) when heated to 245 °C. This weight loss can be attributed to the removal of water that was absorbed on the particles' surface. Additionally, between 250 and 950 °C, there is a further weight loss of 12.76 (wt %) that can be attributed to the formation of hydroxyl groups [49].

As can be seen in the preceding Figure 3c, the thermal resistance of the sample of Cu (INA)$_2$MOF@Fe_3O_4 is quite comparable to that of the [Cu (INA)$_2$]-MOF sample, with only little

Preprints (www.preprints.org) | NOT PEER-REVIEWED | Posted: 23 December 2022 doi:10.20944/preprints202212.0434.v1

differences being brought about by the presence of the [Cu (INA$_2$)-MOF. The fact that the weight loss of [Cu (INA)$_2$]MOF@Fe$_3$O$_4$ is more efficient than that of Cu (INA)$_2$]-MOF at temperatures ranging from 245 to 435 °C demonstrates that the MOF accelerates the degradation of the Fe$_3$O$_4$, which in turn impacts the thermal stability of the materials. In any regard, it is likely that the material that is produced will be utilised at temperatures that are lower.

The XRD used in determining the [Cu(INA)$_2$]-MOF's crystallinity properties showed a high-intensity peaks seen in the spectrum at angles 2θ 10.76 and 22.5, while the hkl of 100 and 200 were respectively obtained (Figure 4a), and they coincided with the XRD pattern previously described for the [Cu(INA)$_2$]-MOF produced by the mechanochemical method [67] [62]. The diameters of the sub-micrometer crystallites that make up the peak in a diffraction pattern are calculated using the Scherrer equation (eqn. 16) [68].

$$\mathbf{D = 1 + \frac{K\lambda}{\beta \cos \theta}} \tag{16}$$

Where: D is the mean size of the ordered (crystalline) domains, K is a dimensionless shape factor, λ is the wavelength and β is the line broadening at half the maximum intensity (FWHM), after subtracting the instrumental line broadening, θ is the Bragg constant calculate the crystallites size of the [Cu (INA)$_2$]-MOF was found to be 39.78 nm.

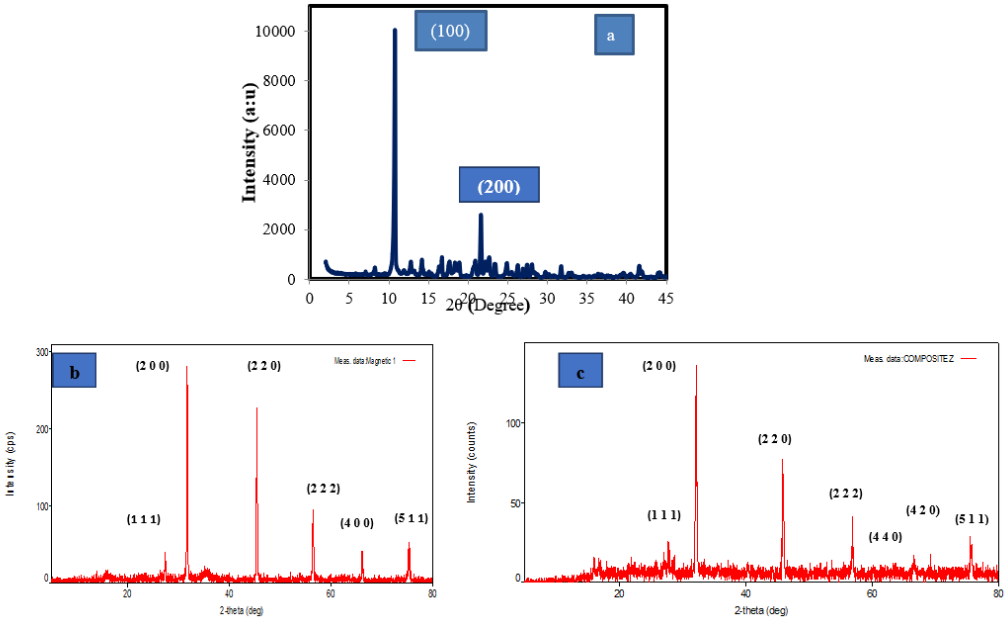

Figure 4. XRD pattern of a) [Cu (INA)$_2$]-MOF b) Fe$_3$O$_4$-MNPs c) [Cu (INA)$_2$]-MOF@Fe$_3$O$_4$.

Note that; It is usual for nanocrystallites to have a high noise level, especially the one observed in the magnetic composite MOFs [69].

Figures 4b, and 4c above display the powder X-ray diffraction (PXRD) patterns of Fe$_3$O$_4$-MNPs, and [Cu (INA)$_2$]-MOF@Fe$_3$O$_4$. The Fe$_3$O$_4$-MNPs PXRD pattern's wide peaks in the diffractogram indicate that the crystallites are nanometric in size. Magnetite, Fe$_3$O$_4$, can't be fully ruled out, although the pattern corresponds quite well with the cubic symmetry of maghemite, Fe$_2$O$_3$ (PDF card 39-1346). Smaller Fe$_3$O$_4$-MNPs are unstable and can transform into maghemite when exposed to oxygen. Due to their identical cell dimensions and shared spinel crystal structure, magnetite and maghemite are difficult to distinguish using X-ray diffraction. The details of each value for the XRD patterns were shown in Table 2. The XRD patterns for the Fe$_3$O$_4$-MNPs and the [Cu (INA)$_2$]-MOF@Fe$_3$O$_4$ revealed five and six distinctive peaks including the hkl indices respectively. The hkl indices are (1 1 1), (2 0 0), (2 2 0), (4 0 0), (5 1 1), found in both the Fe$_3$O$_4$-

Preprints (www.preprints.org) | NOT PEER-REVIEWED | Posted: 23 December 2022 doi:10.20944/preprints202212.0434.v1

MNPs and[Cu (INA)$_2$]-MOF@Fe_3O_4 with an additional (4 2 0) for the [Cu (INA)$_2$]-MOF@Fe_3O_4 this observation clearly indicate an additional compound in the material. The same case was reported by Duan [70] emphasizing that functionalization of a MOFs would not have much effect in the XRD patterns that could cause any considerable change. Based on the results, nanoparticles with a spinel magnetite crystal structure were earlier produced using the mechanochemical process [71], as opposed to other methods, including coprecipitation under ultrasonication, exhibit superior crystallinity, according to a Bellusci [49] study. The tiny size of the crystallites is likely to be the cause of the peak profiles being larger and overlapping when compared to the conventional material, as seen by the XRD profile. [Cu (INA)$_2$]-MOF@Fe_3O_4 exhibits Fe_3O_4-MNPs peaks in its diffraction profile. The clear and absence of impurity peaks shows that the synthesis of the magnetic composite was successful.

In the SEM images, the crystalline phase of the mechanically generated [Cu (INA)$_2$]-MOF at different magnifications with well-defined edges are given in Figure 5a,5b, 5c. The porous nature of [Cu (INA)$_2$]-MOF is facilitated by its morphology, which consists of rectangular-square bars with a rough surface. The surface elemental analysis of the [Cu (INA)$_2$]-MOF in Figure 5d, consists of Cu (13.93), C (48.41), N (13.05), and O (24.61) disclosed by EDX; the obtained images match the composition of the previously published [Cu (INA)$_2$]-MOF [72] [73]. In addition, it was established that the [Cu (INA)$_2$]-MOF@Fe_3O_4 images showed extremely distinct morphological and topological features as shown in Figures 5e, 5f, while Figure 5g presented an in-depth surface morphology of the Fe_3O_4-MNPs with cavities at the outer surface and the elemental representations of the predicted elements in the material as revealed by EDX analysis presented in 5h.

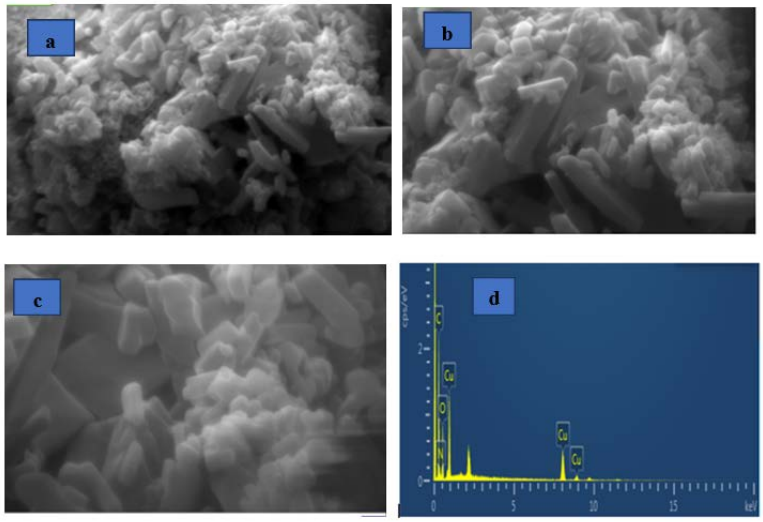

Figure 5. SEM images [Cu (INA)$_2$]-MOF a) scanned at 3.00 magnification b) scanned at 5.00 magnification c) scanned at 10.00 magnification d) EDX surface elemental result

Table 1. EDX of elemental presentation of the [Cu (INA)$_2$]-MOF

Serial number	Elements	Weight %
1	Carbon	49.8
2	Copper	21.3
3	Oxygen	21.7
4	Nitrogen	7.2
Total		100

Preprints (www.preprints.org) | NOT PEER-REVIEWED | Posted: 23 December 2022 doi:10.20944/preprints202212.0434.v1

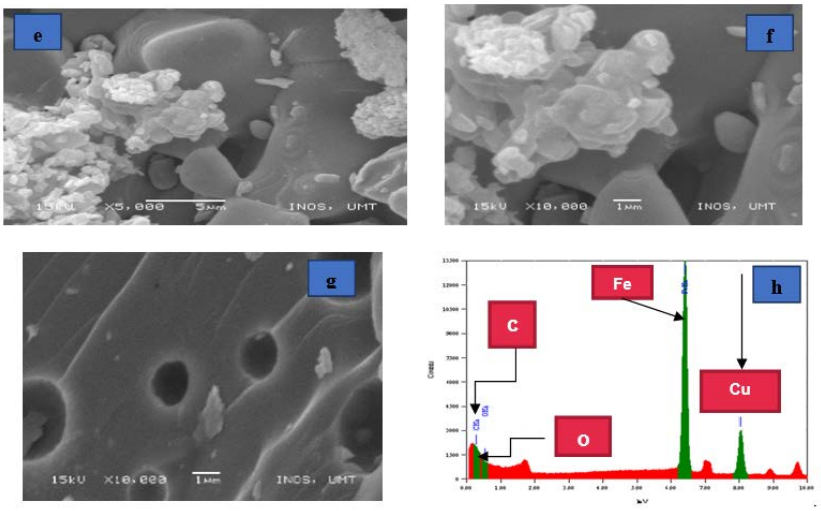

Figure 5. SEM images of samples of [Cu(INA)$_2$]MOF@Fe_3O_4 at e) 5.00 at 5 µm magnification (f) 10.00 at 5 µm magnification g) magnetic iron oxide at10.00 at 5 µm magnification h) EDX Spectrums of the [Cu (INA)$_2$]-MOF@Fe_3O_4.

Table 2. EDX of the elemental representation in the [Cu (INA)$_2$]-MOF@Fe_3O_4 material

Element	Mass %	At %	Compound	Mass %	Cation
C	0.14	0.82	C	0.14	0.00
O	21.59				
Fe	54.41	71.58	FeO	69.99	17.32
Cu	23.86	27.60	CuO	29.87	6.68
Total	100.00	100.00		100.00	24.00

Brunauer-Emmet-Teller (BET) surface areas (SBET) and porosity of [Cu (INA)$_2$]-MOF, Fe_3O_4-MOF, and Cu (INA)$_2$MOFs@Fe_3O_4. The [Cu (INA)$_2$]-MOF was determined by N_2 adsorption tests conducted in liquid nitrogen. And was the value of 20.4 m^2/g The measured SBET for Fe_3O_4-MNPs was 25.3 m^2/g, while the (Cu (INA)$_2$MOFs@Fe_3O_4) was 27.2 m^2/g, which is consistent with the results of the XRD study and represents an equivalent diameter size of approximately 4 nm. Our new adsorbent synthesized in our laboratory was shown to have better a better surface area than the Fe_3O_4-MNPs and its composites synthesized by Aryee [74] with 0.29 m^2/g, 0.40 m^2/g and 10.45 m^2/g in their different synthesis.

3.2 Removal Studies

3.2.1 Effect of contact time

For adsorption studies to gain a comprehensive understanding of the equilibrium condition, the influence of contact time must be considered. Terbutaline adsorption onto [Cu (INA)$_2$]-MOF and [Cu (INA)$_2$]-MOF@Fe_3O_4 was studied at 25 °C, an optimum pH of 11, and adsorbate concentrations of 40 mg L^{-1}. Effect of contact time is illustrated in Figure 6 on the removal of terbutaline. The results demonstrated the effective removal of terbutaline in the first stage of the process, reaching equilibrium in all adsorption studies using both adsorbents in around 40 minutes. The quicker removal of the pollutant can be attributed to the favourable interactions of terbutaline molecule with the adsorbents due to the availability of some functional groups (- OH and - N) as well as the added magnetic properties that characterise the modified [Cu (INA)$_2$]-MOF@Fe_3O_4, which are favourable adsorption sites present on the surface of the adsorbents [61]. To guarantee the MOF's efficiency under the equilibrium condition, the adsorption was prolonged till 120 minutes, a very good removal efficiencies of 92 and 99 % were recorded and no

Preprints (www.preprints.org) | NOT PEER-REVIEWED | Posted: 23 December 2022 doi:10.20944/preprints202212.0434.v1

any further observable progress were observed after reaching the 40 minutes contact time. This result was consistent with the results of other adsorption investigations [40].

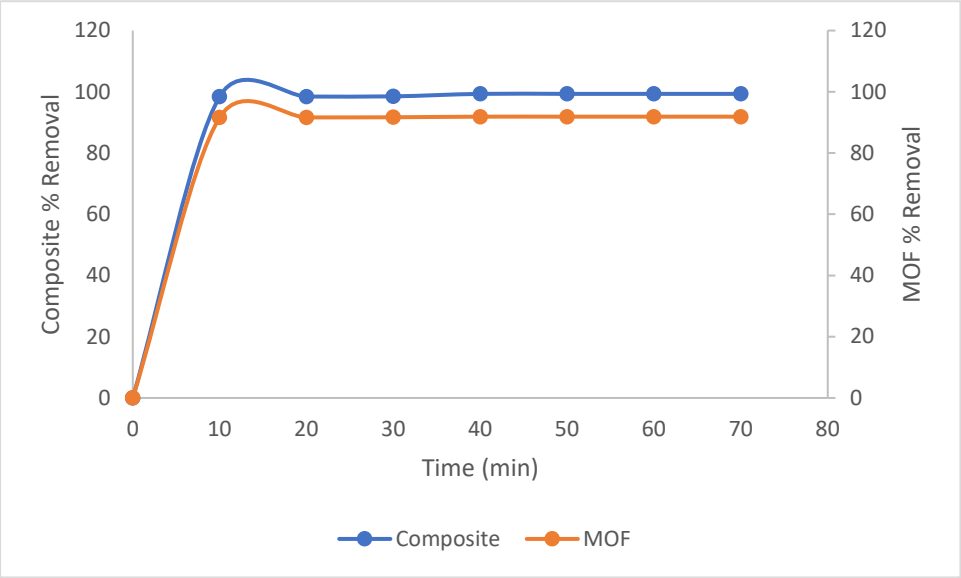

Figure 6. Effect of contact time for the [Cu (INA)$_2$]-MOF and [Cu (INA)$_2$]-MOF@Fe_3O_4

3.2.2 Effect of terbutaline initial concentration

Adsorption studies were carried out to investigate the effect of terbutaline initial concentrations ranging from 10 to 60 mg L^{-1}. Figure 7 depicted the effect of the initial terbutaline concentration on the adsorption, which rose as the terbutaline concentrations increased. The results showed that terbutaline removal for both the adsorbents was approximately 91.8% and 99.3% with initial concentration of 40 mg L^{-1} for both the [Cu (INA)$_2$]-MOF and [Cu (INA)$_2$]-MOF@Fe_3O_4 at the lowest dosage of 1 mg g^{-1} in all the adsorbates studied, respectively. These results showed that both [Cu (INA)$_2$]-MOF and [Cu (INA)$_2$]-MOF@Fe_3O_4 had good removal efficiencies with the [Cu (INA)$_2$]-MOF@Fe_3O_4 having the highest removal efficiency which can be attributed to the magnetic modification on the material. Isiyaka reported the same phenomenon in his removal investigation on dicamba using composite-MOF [40].

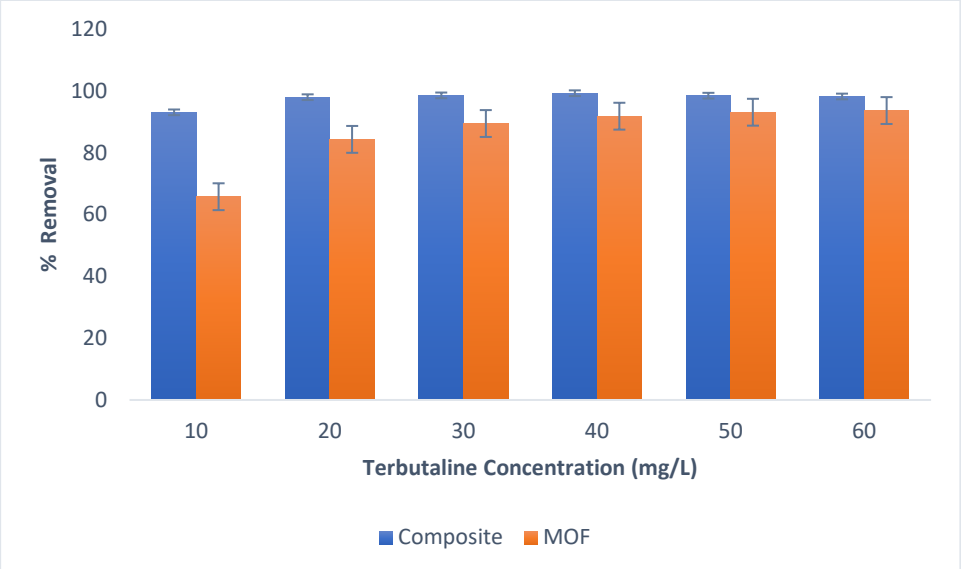

Preprints (www.preprints.org) | NOT PEER-REVIEWED | Posted: 23 December 2022 doi:10.20944/preprints202212.0434.v1

Figure 7. Terbutaline Initial Concentration for the [Cu (INA)$_2$]-MOF and [Cu (INA)$_2$]-MOF@Fe_3O_4

3.2.3 Effect of MOF dosage

For an adsorbent material to be considered suitable for usage, it must achieve maximal adsorption effectiveness even at the lowest possible dosage and in the shortest time possible [56]. Thus, the impact of both adsorbent doses for terbutaline adsorption was investigated in the range of 1–6 mg g^{-1}, in a 40 mL solution having adsorbate concentrations in the ranges of 40 mg L^{-1}, at an ideal alkaline pH of 11 at 25 °C. It can be observed from Figure 8 that, the quantity of terbutaline adsorbed is varied with varying adsorbent mass and decrease with increase in adsorbent mass. The quantity of Terbutaline adsorbed reduces from 1470 mg g^{-1} to 247 mg g^{-1} for the 1589 mg/g to 264 mg/g for [Cu (INA)$_2$]-MOF and [Cu (INA)$_2$]-MOF@Fe_3O_4 respectively when the adsorbent mass increases from 1 mg g^{-1} to 6 mg g^{-1}. At higher [Cu (INA)$_2$]-MOF and [Cu (INA)$_2$]-MOF@Fe_3O_4 to solute concentration ratios, there is a rapid superficial adsorption onto the adsorbent surface, resulting in a reduced solute concentration in the solution. This is because a set mass of the adsorbent material can only adsorp a certain quantity of terbutaline. Therefore, the higher the adsorbent dose, the greater the amount of effluent that can be purified by a certain mass of MOFs. Due to the split in the flux or the concentration gradient between the solute concentration in the solution and the solute concentration on the surface of the adsorbent, the quantity of terbutaline adsorbed qe (mg/g) decreases with increasing adsorbent mass. Thus, when adsorbent mass increases, the quantity of terbutaline absorbed per unit weight of adsorbent decreases, resulting in a drop in qe value as adsorbent mass concentration increases. Studies using various adsorbents demonstrates the same scenario [75] [76] and in a very recent research by Aryee [74]. This property is primarily explained by the fact that adsorption sites stay unsaturated during the adsorption reaction, but the number of available adsorption sites rises as the adsorbent dosage increases.

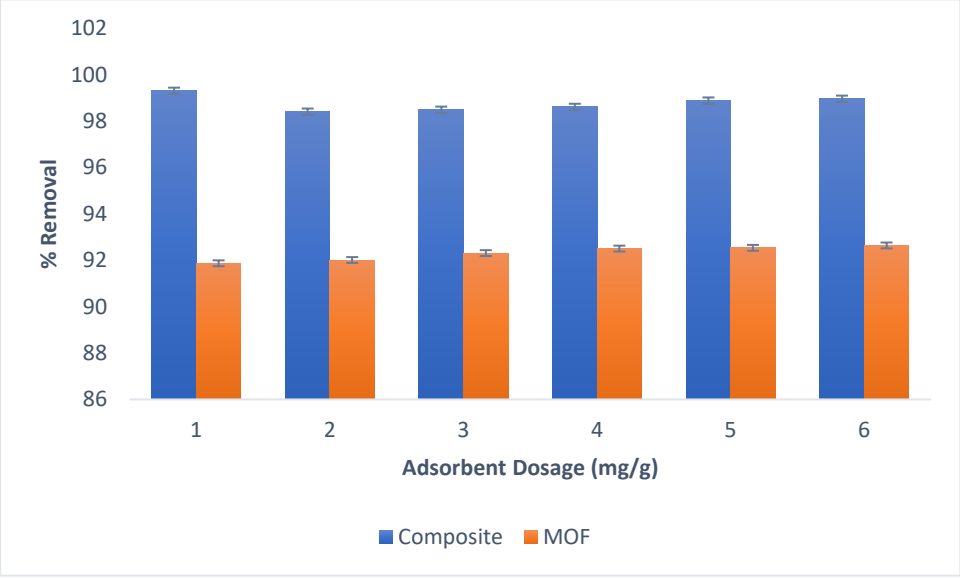

Figure 8. Effect of [Cu (INA)$_2$]-MOF and [Cu(INA)$_2$]-MOF@Fe_3O_4 dosages

It was also discovered that the adsorption capacity of terbutaline adsorbed onto [Cu (INA)$_2$]-MOF and [Cu(INA)$_2$]-MOF@Fe_3O_4 differs between the two adsorbents, with the [Cu(INA)$_2$]-MOF@Fe_3O_4)-MOF possessing an excellent adsorption capacity of more than 1500 mg g^{-1}

3.2.4 Effect of pH

Preprints (www.preprints.org) | NOT PEER-REVIEWED | Posted: 23 December 2022 doi:10.20944/preprints202212.0434.v1

The influence of pH on terbutaline adsorption onto the [Cu (INA)$_2$]-MOF and [Cu(INA)$_2$]-MOF@Fe_3O_4 were studied at pH levels of 3, 5, 7, 9, 11, and 13. The results indicate that the pH of the solution has a significant impact on the performance of both [Cu(INA)$_2$]-MOF and [Cu(INA)$_2$]-MOF@Fe_3O_4 for terbutaline adsorption, as shown in Figure 9. Terbutaline is a tertiary amine with an acidity constant (pKa) of 9.12, hence its species are generally positively charged in solution at pH ranging from 3 to 9. As the pH of the solution increased, adsorption efficiency was observed to improve up to pH 11 with a very excellent percentage removal of over 92 % and 99 % in both the [Cu (INA)$_2$]-MOF and [Cu (INA)$_2$]-MOF@Fe_3O_4, indicating that this phenomenon favors the adsorption process. Selkälä [34] highlighted how ionizable contaminants react with changes in pH and colloidal stability using a member of β-agonist compound as case study.

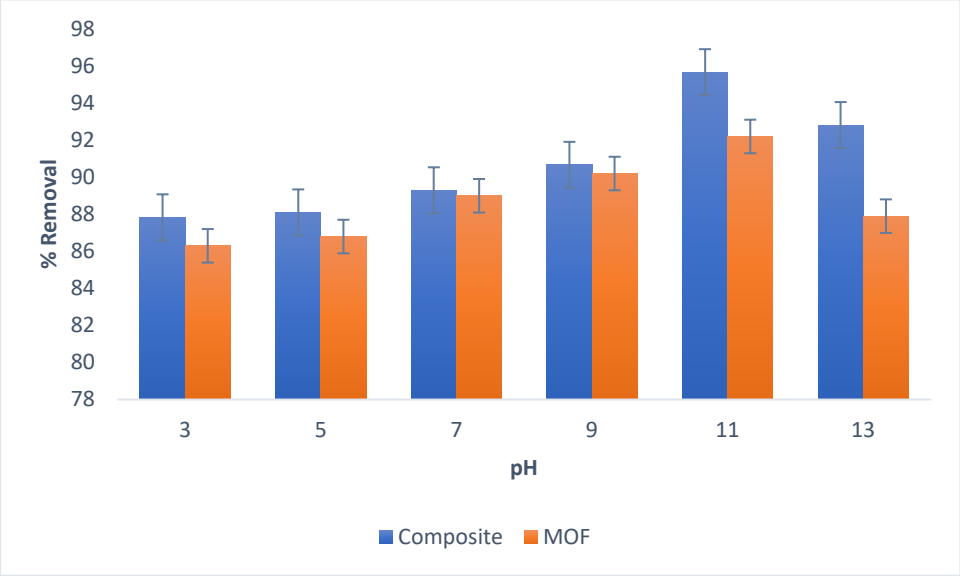

Figure 9. pH Effect of the [Cu (INA)$_2$]-MOF and [Cu (INA)$_2$]-MOF@Fe_3O_4 on terbutaline adsorption

3.2.5 Kinetics of the adsorption studies

The interaction between the pollutants (analyte) and the surface of the adsorbent materials determines the adsorption of pollutants onto the adsorbents. The interaction between the terbutaline and the surface of the [Cu (INA)$_2$]-MOF and [Cu (INA)$_2$]-MOF@Fe_3O_4 materials determines the adsorption of terbutaline onto the as-synthesized adsorbents. To determine the best fitting for the adsorption mechanism, the kinetics of the process from the effect of adsorbent dosage was computed with the effect of contact time. In the kinetic models the adsorption data according to the statistical values highlighted in Table 3 for both the [Cu (INA)$_2$]-MOF and the [Cu (INA)$_2$]-MOF@Fe_3O_4 indicated strong fitness on the pseudo-second-order values of the parameters as it was shown to better explain the adsorption data in terms of greater R^2, adj R^2 as well as both lower RMSE and AIC values, than the rest of the two tested and compared models. The measured/calculated qe (mg g^{-1}) values also correspond with the results of the experimental qe (mg g^{-1}) values on both the [Cu (INA)$_2$]-MOF and [Cu (INA)$_2$]-MOF@Fe_3O_4 (the graphical representations are presented in the supplementary materials section). It was determined that the higher adsorption efficiency of the composite material towards the β-agonists adsorption from the aqueous phase was due to the availability of abundant adsorption sites on the surface of the MOF. This was agreed upon evidently seen from the BET surface area and for volume analysis of the [Cu (INA)$_2$]-MOF@Fe_3O_4. Additionally, it pointed to a process of chemisorption. As a result, greater adsorption of the β-agonists was seen within a shorter amount of time for equilibration. The result was in agreement with the reports of Tang [33] Hamza [77].

Preprints (www.preprints.org) | NOT PEER-REVIEWED | Posted: 23 December 2022 doi:10.20944/preprints202212.0434.v1

Table 3. Comparison of adsorption kinetic parameters for the removal of Terbutaline using [Cu (INA)$_2$]-MOF and [Cu (INA)$_2$]-MOF@Fe_3O_4

Kinetics models	Parameters	[Cu (INA)$_2$]-MOF	[Cu (INA)$_2$]-MOF@Fe_3O_4
Pseudo first order	q_{exp} (mg g $^{-1}$)	1470	1589.124
	q_{cal} (mg g $^{-1}$)	2.718	3.530
	K_1	0.026	0.0458
	R^2	0.3026	0.040
	R^2adj	0.802	0.320
	RMSE	1.229	29.99
	AIC	2.875	49.26
Pseudo second order	q_{exp} (mg g $^{-1}$)	1470	1589.124
	q_{cal} (mg g $^{-1}$)	1428	2500
	K_2 (mg g $^{-1}$ min $^{-1}$)	4.9039	0.2
	R^2	1	1
	R^2adj	0.900	1
	RMSE	0.009	0.001
	AIC	-64.41	-92.87
Intraparticle Diffusion	K_P (mg g $^{-1}$ min $^{-1}$)	12.316	19.683
	C	1030.8	1657.3
	R^2	0.1987	0.199
	R^2adj	0.080	0.362
	RMSE	3.261	14.53
	AIC	20.6	39.12

3.2.6 Isotherm Studies

The surface interaction of both the [Cu (INA)$_2$]-MOF and [Cu (INA)$_2$]-MOF@Fe_3O_4 with the terbutaline molecules at the equilibrium of the process was studied by 3 prominent Isotherm models as mentioned earlier: namely, the Langmuir, Freundlich, and Temkin models. Both the [Cu (INA)$_2$]-MOF and [Cu (INA)$_2$]-MOF@Fe_3O_4 followed the same pattern of adsorption characteristics as shown from the comparison adsorption data in Table 4. Langmuir model was discovered to have the best fitting of all the isotherms models of the two adsorbents, with the highest R^2 of 0.8949, Adj. R^2 of 0.877, with RMSE of 0.011, and a least AIC value of -52.946 in the [Cu (INA)$_2$]-MOF and in the [Cu (INA)$_2$]-MOF@Fe_3O_4 the same Langmuir model is also best fit with the highest R^2 of 0.9994, Adj R^2 of 0.710, with RMSE of 0.004, and a least AIC value of -76.903 Based on the above findings, it could be concluded that the Langmuir model better reflects the experimental data and is the best model for all the adsorbents in the current research. Tang [33] observed the same scenario when he explored the ability of molecularly imprinted polymer using covalent imprinting technique in the determination of a β-agonist compound in a portable water sample. The Langmuir results also demonstrates that the [Cu (INA)$_2$]-MOF and the [Cu (INA)$_2$]-MOF@Fe_3O_4 forms homogeneous adsorption sites on the adsorption surface suggesting the formation of a monolayer contact with the terbutaline molecule. The results also shows that there is limited number of adsorption sites available in the [Cu (INA)$_2$]-MOF and the [Cu (INA)$_2$]MOF@Fe_3O_4 for the adsorption of the analytes and that the attractive forces decrease with increasing distances. On comparison between the two adsorbents the [Cu (INA)$_2$]-MOF@Fe_3O_4

Preprints (www.preprints.org) | NOT PEER-REVIEWED | Posted: 23 December 2022 doi:10.20944/preprints202212.0434.v1

shows the best results in all the parameters with the better q_m value of 2500 as compared to 1666.67 in [Cu (INA)$_2$]-MOF.

Table 4. Comparison of Isotherm parameters for adsorption of Terbutaline onto the [Cu (INA)$_2$]-MOF and the [Cu (INA)$_2$]-MOF@Fe_3O_4

Isotherm models	Parameters	[Cu (INA)$_2$]-MOF	[Cu (INA)$_2$]-MOF@Fe_3O_4
Langmuir	q_m (mg/g)	1666.67	2500
	K_L (L/mg)	0.00059	0.00175
	R_L	0.976	0.09
	R^2	0.8593	0.9994
	R^2adj	0.877	0.710
	RMSE	0.011	0.004
	AIC	-52.946	-76.903
Freundlich	K_F (L/g)	2.718	2.1555
	N	0.1894	0.00692
	R^2	0.8541	0.8872
	R^2adj	0.869	0.737
	RMSE	0.039	0.007
	AIC	-37.341	-68.452
Temkin	A (L/g)	1.0009	1.0053
	b_T (kJ/mol)	1090.8	43965
	R^2	0.858	0.8779
	R^2adj	0.827	0.667
	RMSE	4.662	0.006
	AIC	23.199	-70.005

3.2.7 Effect of temperature and thermodynamic studies

The temperature studies and thermodynamics analysis for the adsorption of terbutaline onto both the [Cu (INA)$_2$]-MOF and the [Cu (INA)$_2$]-MOF@Fe_3O_4 adsorbents were conducted by varying the temperature in the range of 25, 30, 35, 40, 45, and 50 °C i.e., 298, 303, 308, 313, 318 and 323 K using batch experiments. The result is presented in Figure 10 and it shows a decrease in the removal efficiencies for both the [Cu (INA)$_2$]-MOF and [Cu (INA)$_2$]-MOF@Fe_3O_4 from 92 % to 67 % and 97 % to 74 % as the temperature rose from 25 to 50 °C (298 K to 388 K) respectively, indicating that the mechanism was an endothermic one [78]. Temperature increases reduce the contact between the adsorbate and adsorbent molecules, indicating physisorption [79]. The result as presented shows the adsorption capacity of terbutaline decreases with increasing temperature. Using the thermodynamic model and parameters, the adsorption was shown to be SPONTANEOUS, according to the negative values of $\Delta G°$ obtained as the temperature increased the reaction occur without any energy input [78]. This result shows that the adsorption is unfavorable at higher temperature, it is also endothermic according to the positive values of enthalpy change ($\Delta H°$) obtained which specified that the products in the reaction have more energy compared to the reactants, so the reaction has gained energy, making it endothermic, while according to the positive value of $\Delta S°$ obtained which is the degree of randomness at the solid/liquid interface as well as structural changes in the adsorbent and adsorbate, and the process of adsorption is validated as chemisorption. It also indicates the affinity of the adsorbent for the adsorbate.

Preprints (www.preprints.org) | NOT PEER-REVIEWED | Posted: 23 December 2022 doi:10.20944/preprints202212.0434.v1

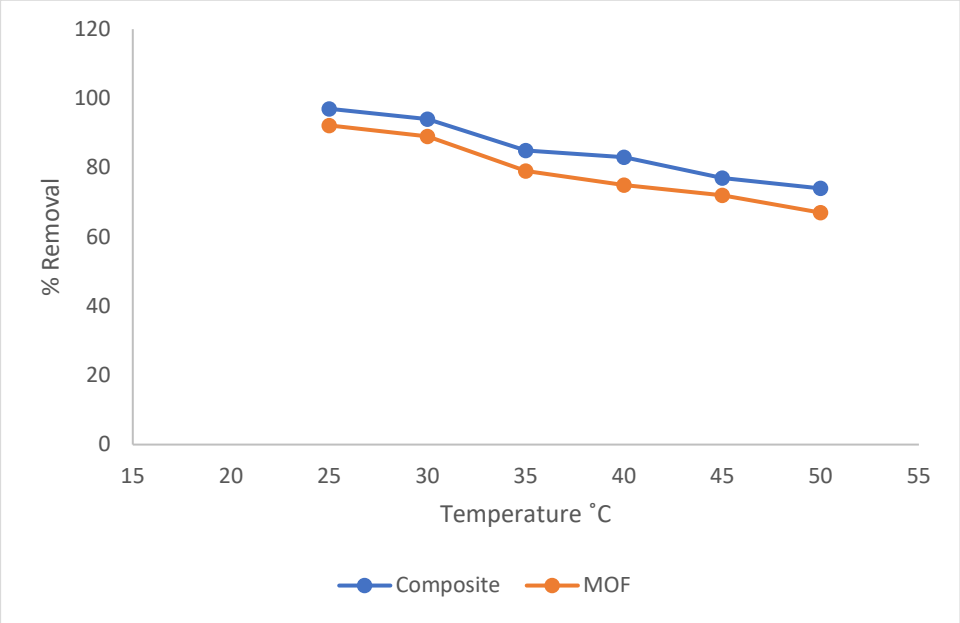

Figure 10. Effect of temperature on the adsorption of Terbutaline on both the [Cu (INA)$_2$]-MOF and [Cu (INA)$_2$]-MOF@Fe_3O_4

Table 5. Thermodynamic Parameters for the adsorption of terbutaline onto [Cu (INA)$_2$]-MOF$^{\#}$ and [Cu (INA)$_2$]-MOF@Fe_3O_4

Temp (K)	ΔG°$^{\#}$ (kJ/mol)	ΔG°* (kJ/mol)	ΔH° (KJ/mol)	ΔS° (J/mol/K)
298	-0.5640	-0.03814		
303	-0.5735	-0.03878		
308	-0.5829	-0.03942	0.00582*	0.1280*
313	-0.5924	-0.04006	0.072$^{\#}$	1.8930$^{\#}$
318	-0.6019	-0.04070		
323	-0.6111	-0.04134		

$^{\#,*}$ Indicate values from the [Cu (INA)$_2$]-MOF and [Cu (INA)$_2$]-MOF@Fe_3O_4 respectively

3.2.8 Adsorbent Regeneration and Reusability

Five complete batch adsorption cycles were used to evaluate the ease of [Cu (INA)$_2$]-MOF and [Cu (INA)$_2$]-MOF@Fe_3O_4 recovery following active batch adsorption as an indicator of their potential as adsorbents for the removal of terbutaline. Thus, the adsorbents were regenerated according to the method described in section 2.6.2, and adsorption was conducted in a 40 mL solution containing an adsorbate concentration of 40 mg L^{-1} at an optimal alkaline pH of 11 with a contact time of 40 minutes, as previously determined for both respective adsorbents. Following batch adsorption studies, the removal efficiency for adsorption cycles was recorded. As shown in Figure 11, the adsorption removal efficiencies for the two adsorbents ranges from 91.8 % down to 85 % for the [Cu (INA)$_2$]-MOF and from 99.3 % to 94.7 % for the [Cu (INA)$_2$]-MOF@Fe_3O_4 respectively. Higher percentage values indicated the good reusability of both adsorbents for the adsorption of terbutaline from environmental waters even after subsequent regenerations. Isiyaka [40] and Zango [78] obtained comparable outcomes in utilizing two different adsorbents.

Preprints (www.preprints.org) | NOT PEER-REVIEWED | Posted: 23 December 2022 doi:10.20944/preprints202212.0434.v1

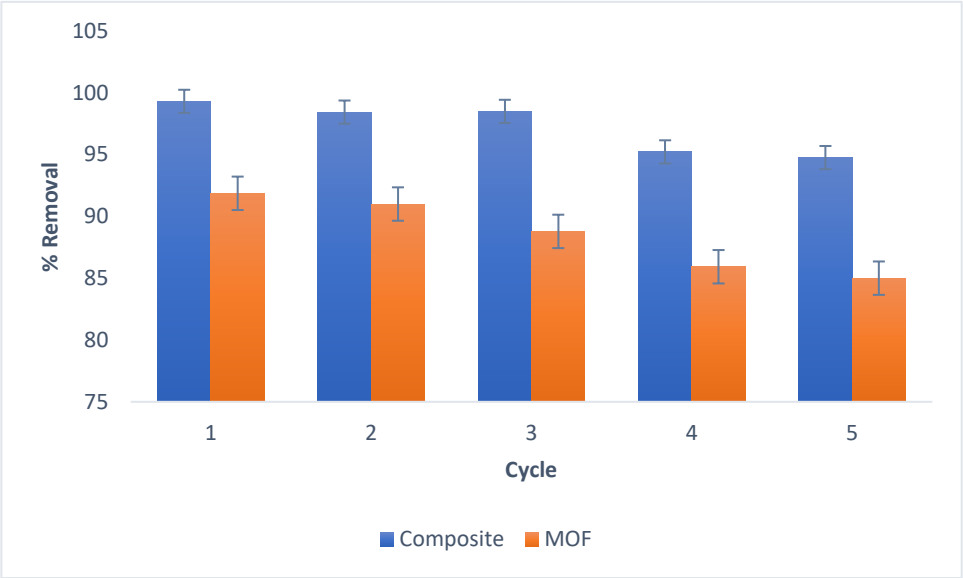

Figure 11. Regeneration and Reusability of [Cu (INA)$_2$]-MOF and [Cu (INA)$_2$]-MOF@Fe_3O_4

3.2.9 Comparison studies

Due to a shortage of related data in the reported literature on the removal of terbutaline and other β-agonists in general, a comparison was made between the relevant characteristics' adsorbents used for the removal of β-agonists in water and our reported adsorbents as well. Table 4 demonstrates that our study using [Cu (INA)$_2$]-MOF and [Cu (INA)$_2$]-MOF@Fe_3O_4 have some significantly greater removal percentage of 91.8 % and 99.3 %, a considerable equilibrium time, and the benefit of easily regenerating the adsorbent, which has not been addressed in many of the reported articles and some of the studies did not provide the maximum adsorption capacity (Q_{max}) of their adsorption, although accurate comparisons are not possible due to the variance in experimental and laboratory settings employed by the experts.

Table 6. ***Adsorbents reported for the removal of β-agonists from water***

Adsorbent materials	Equilibrium time	Q_{max} (mg g^{-1})	% Removal	Analytes	Reference
μ-Grain Activated Carbon	48 hours	N.A	78.6	Salbutamol	[31]
MIP@UCPs prove	20 min	2.18	81.7	Clenbuterol	[32]
MIP@CIP	20 min	7.34	74.0	Clenbuterol	[33]
Granular Activated Carbon	Not provided	N.A	83.0	Salbutamol	[17]
Ui-66 MOF	60 min	160	80.0	Clenbuterol	[42]
ED-MIL-101(Cr)	Not provided	N.A	90.1	Terbutaline	[45]
[Cu (INA)$_2$]-MOF	40 minutes	1666.67	92.0	Terbutaline	This study
[Cu (INA)$_2$]-MOF@Fe_3O_4	40 minutes	2500	99.0	Terbutaline	This study

5. Conclusions

The adsorptive removal of terbutaline from the water was achieved through the mechanochemical production of [Cu (INA)$_2$]-MOF and its magnetic composite [Cu (INA)$_2$]-MOF@Fe_3O_4. Fourier transform infrared spectroscopy (FTIR), thermogravimetric

analysis (TGA), X-ray diffraction (XRD), and scanning electron microscopy (SEM) were all used to highlight the unique characteristics of the two advanced materials and were studied as adsorbents for extensive Terbutaline removal in water. Parameters influencing the adsorption studies like Contact time, starting Terbutaline concentration, pH, and temperature were all explored in detail to determine the best adsorption conditions, using Kinetics, isotherms, and thermodynamics as well as other aspects of the adsorption process like the regeneration studies to assess the adsorbents' reusability were all investigated. The magnetic iron composite [Cu (INA)$_2$]-MOF@Fe_3O_4 exhibited better favorable characteristics, achieving an exceptional adsorption capacity of 1589 mg g^{-1} with Q_{max} of 2500 mg g^{-1} than [Cu (INA)$_2$]-MOF with 1470 mg g^{-1} and 1666.67 mg g^{-1}. Alkaline pH has a great influence for the adsorption of terbutaline in both the adsorbents. The best model from the kinetics study was a non-uniform pseudo-second order adsorption process in both the two materials which was determined according to the statistical fittings of higher R^2, and adj. R^2 values, and lower RMSE, and AIC values. The Langmuir model was the best fit in Isotherm models in all the two materials too from the statistical fittings with higher R^2, and adj. R^2 values, and lower RMSE, and AIC. The effect of temperature shows an endothermic process, with the spontaneous nature of the process based on the $\Delta G°$ and an increase randomness in the solid-liquid interface. The successive removal of the pollutant for 5 cycles, achieving good adsorption removal of up to 85 % and 95 % in the [Cu (INA)$_2$]-MOF and [Cu (INA)$_2$]-MOF@Fe_3O_4, demonstrated the good reusability and prospective effectiveness of both the materials with the [Cu (INA)$_2$]-MOF@Fe_3O_4 showing a superior and better values in all the adsorption parameters for terbutaline adsorption.

Author Contributions: "Conceptualization, U.A. and M.M.A.; methodology, U.A.; software, H.M.Y.; validation, S.H.L., H.M.Y. and W.M.A.; formal analysis, U.A.; investigation, U.A.; resources, M.M.A.; data curation, H.M.Y and W.M.A.; writing—original draft preparation, U.A.; writing—review and editing, M.M.A. S.H.L H.M.Y and W.M.A; visualization, U.A and S.H.L.; supervision, M.M.A and H.M.Y.; project administration, M.M.A.; funding acquisition, M.M.A. All authors have read and agreed to the published version of the manuscript."

Funding: This research project was supported by Al-Qalam University Katsina, Nigeria and Universiti Malaysia Terengganu (Postgraduate Research Grant Vot. No. 55202)

Acknowledgments: The authors would like to acknowledge the technical supports and advise from Dr. Zakariyya and Dr. Hamza from Universiti Technologi Petronas (Malaysia).

Conflicts of Interest: The authors declare no conflict of interest.

References

[1] L. Mohammadi *et al.*, "Removal of Amoxicillin from Aqueous Media by Fenton-like Sonolysis/H2O2 Process Using Zero-Valent Iron Nanoparticles," *Molecules*, vol. 27, no. 19, pp. 1–13, 2022, doi: 10.3390/molecules27196308.

[2] G. Zhao *et al.*, "Magnetic Nanoparticles@Metal-Organic Framework Composites as Sustainable Environment Adsorbents," *Journal of Nanomaterials*, vol. 2019. Hindawi Limited, 2019. doi: 10.1155/2019/1454358.

[3] C. Hignite and D. L. Azarnoff, "Drugs and drug metabolites as environmental contaminants: Chlorophenoxyisobutyrate and salicylic acid in sewage water effluent," *Life Sci.*, vol. 20, no. 2, pp. 337–341, 1977, doi: 10.1016/0024-3205(77)90329-0.

[4] M. Gavrilescu, K. Demnerová, J. Aamand, S. Agathos, and F. Fava, "Emerging pollutants in the environment: present and future challenges in biomonitoring, ecological risks and bioremediation," *N. Biotechnol.*, vol. 32, no. 1, pp. 147–156, Jan. 2015, doi: 10.1016/j.nbt.2014.01.001.

[5] U. Armaya'u, M. M. Ariffin, S. H. Loh, W. M. A. W. Mohd Khalik, and H. M. Yusoff, "β-Agonist in the environmental waters: a review on threats and determination methods," *Green Chem. Lett. Rev.*, vol. 15, no. 1, pp. 232–251, Jan. 2022, doi: 10.1080/17518253.2022.2032843.

[6] Z. Li, Chenglong. Li, Jingya. Jiang, Wenxiao. Zhang, Suxia. Shen, Jianzhong. Wen, Kai. Wang, "Development and Application of a Gel-based Immunoassay for Rapid Screening of Salbutamol and Ractopamine Residues in Pork," *J. Agric. Food Chem.*, vol. 63, pp. 10556–10561, 2015, doi: 10.1021/acs.jafc.5b04203.

[7] M. Hemmati, M. Rajabi, and A. Asghari, "Ultrasound-promoted dispersive micro solid-phase extraction of trace anti-hypertensive drugs from biological matrices using a sonochemically synthesized conductive polymer nanocomposite," *Ultrason. Sonochem.*, vol. 39, pp. 12–24, 2017, doi: 10.1016/j.ultsonch.2017.03.024.

[8] J. Pilcher *et al.*, "Beta-agonist overuse and delay in obtaining medical review in high risk asthma: a secondary analysis of data from a randomised controlled trial," *npj Prim. Care Respir. Med.*, vol. 27, no. 1, p. 33, Dec. 2017, doi: 10.1038/s41533-017-0032-z.

[9] D. P. Tashkin and L. M. Fabbri, "Long-acting beta-agonists in the management of chronic obstructive pulmonary disease: Current and future agents," *Respir. Res.*, vol. 11, pp. 1–14, 2010, doi: 10.1186/1465-9921-11-149.

[10] W. E. Cayley, "Beta2 Agonists for Acute Cough or a Clinical Diagnosis of Acute Bronchitis," *Am. Fam. Physician*, vol. 95, no. 9, pp. 551–552, 2017, doi: 10.1002/14651858.CD001726.pub5.Copyright.

[11] T. Simmons and E. Blazar, "Synergistic Bradycardia from Beta Blockers, Hyperkalemia, and Renal Failure," *J. Emerg. Med.*, vol. 57, no. 2, pp. e41–e44, 2019, doi: 10.1016/j.jemermed.2019.03.039.

[12] M. Li *et al.*, "Ultrasensitive and Quantitative Detection of a New β - Agonist Phenylethanolamine A by a Novel Immunochromatographic Assay Based on Surface-Enhanced Raman Scattering (SERS)," *J. Agric. Food Chem.*, vol. 62, p. 10896–10902, 2014, doi: 10.1021/jf503599x.

[13] G. Barisione, M. Baroffio, E. Crimi, and V. Brusasco, "Beta-Adrenergic Agonists," *Pharmaceuticals*, vol. 3, no. 4, pp. 1016–1044, Mar. 2010, doi: 10.3390/ph3041016.

[14] V. S. Fan *et al.*, "Overuse of short-acting beta-agonist bronchodilators in COPD during periods of clinical stability," *Respir. Med.*, vol. 116, pp. 100–106, 2016, doi: 10.1016/j.rmed.2016.05.011.

[15] L. Xu, X. Qi, X. Li, Y. Bai, and H. Liu, "Recent advances in applications of nanomaterials for sample preparation," *Talanta*, vol. 146, pp. 714–726, 2016, doi: 10.1016/j.talanta.2015.06.036.

[16] A. A. Salem, I. A. Wasfi, and S. S. Al-Nassibi, "Trace determination of β-blockers and β2-agonists in distilled and waste-waters using liquid chromatography-tandem mass spectrometry and solid-phase extraction," *J. Chromatogr. B Anal. Technol. Biomed. Life Sci.*, vol. 908, pp. 27–38, 2012, doi: 10.1016/j.jchromb.2012.09.026.

[17] D. J. de Ridder *et al.*, "Influence of natural organic matter on equilibrium adsorption of neutral and charged pharmaceuticals onto activated carbon," *Water Sci. Technol.*, vol. 63, no. 3, pp. 416–423, Feb. 2011, doi: 10.2166/wst.2011.237.

[18] PubChem, "PubChem Terbutaline," *https://www.drugbank.ca/drugs/DB00871*, 2021.

[19] H. A. Spiller, K. J. James, S. Scholzen, and D. J. Borys, "A descriptive study of adverse events from clenbuterol misuse and abuse for weight loss and bodybuilding," *Subst. Abus.*, vol. 34, no. 3, pp. 306–312, 2013, doi: 10.1080/08897077.2013.772083.

[20] A. M. Beltagi, H. S. El-Desoky, and M. M. Ghoneim, "Quantification of terbutaline in pharmaceutical formulation and human serum by adsorptive stripping voltammetry at a glassy carbon electrode," *Chem. Pharm. Bull.*, vol. 55, no. 7, pp. 1018–1023, 2007, doi: 10.1248/cpb.55.1018.

[21] N. Žlak, D. Košuta, M. Potisek, and Ž. Stevanović, "Clenbuterol toxicity in a young male athlete," *Toxin Rev.*, vol. 37, no. 3, pp. 182–186, 2018, doi: 10.1080/15569543.2017.1348361.

[22] C. Duan, J. Wang, Q. Liu, Y. Zhou, and Y. Zhou, "Efficient removal of Salbutamol and Atenolol by an electronegative silanized β-cyclodextrin adsorbent," *Sep. Purif. Technol.*, vol. 282, no. PB, p. 120013, 2022, doi: 10.1016/j.seppur.2021.120013.

[23] P. K. Kalambate, C. R. Rawool, and A. K. Srivastava, "Fabrication of graphene nanosheet-multiwalled carbon nanotube-polyaniline modified carbon paste electrode for the simultaneous electrochemical determination of terbutaline sulphate and guaifenesin," *New J. Chem.*, vol. 41, no. 15, pp. 7061–7072, 2017, doi: 10.1039/c7nj00101k.

[24] N. Sakai, M. Sakai, D. E. Mohamad Haron, M. Yoneda, and M. Ali Mohd, "Beta-agonist residues in cattle, chicken and swine livers at the wet market and the environmental impacts of wastewater from livestock farms in Selangor State, Malaysia," *Chemosphere*, vol. 165, pp. 183–190, 2016, doi: 10.1016/j.chemosphere.2016.09.022.

[25] H. Du *et al.*, "Sensitive and specific detection of a new β-agonist brombuterol in tissue and feed samples by a competitive polyclonal antibody based ELISA," *Anal. Methods*, vol. 8, no. 17, pp. 3578–3586, 2016, doi: 10.1039/c6ay00079g.

[26] M. Weil, A. M. Falkenhain, M. Scheurer, J. J. Ryan, and A. Coors, "Uptake and Effects of the Beta-Adrenergic Agonist Salbutamol in Fish: Supporting Evidence for the Fish Plasma Model," *Environ. Toxicol. Chem.*, vol. 38, no. 11, pp. 2509–2519, 2019, doi: 10.1002/etc.4543.

[27] M. Petrović, B. Škrbić, J. Živančev, L. Ferrando-Climent, and D. Barcelo, "Determination of 81 pharmaceutical drugs by high performance liquid chromatography coupled to mass spectrometry with hybrid triple quadrupole-linear ion trap in different types of water in Serbia," *Sci. Total Environ.*, vol. 468–469, pp. 415–428, 2014, doi: 10.1016/j.scitotenv.2013.08.079.

[28] R. Rodil *et al.*, "Emerging pollutants in sewage, surface and drinking water in Galicia (NW Spain)," *Chemosphere*, vol. 86, no. 10, pp. 1040–1049, Mar. 2012, doi: 10.1016/j.chemosphere.2011.11.053.

[29] Y. Lan, C. Coetsier, C. Causserand, and K. Groenen Serrano, "An experimental and modelling study of the electrochemical oxidation of pharmaceuticals using a boron-doped diamond anode," *Chem. Eng. J.*, vol. 333, no. June 2017, pp. 486–494, 2018, doi: 10.1016/j.cej.2017.09.164.

[30] S. Yan *et al.*, "Development of Fluorescence Surrogates to Predict the Photochemical Transformation of Pharmaceuticals in Wastewater Effluents," *Environ. Sci. Technol.*, vol. 51, no. 5, pp. 2738–2747, 2017, doi: 10.1021/acs.est.6b05251.

[31] T. C. Alves, A. Cabrera-Codony, D. Barceló, S. Rodriguez-Mozaz, A. Pinheiro, and R. Gonzalez-Olmos, "Influencing factors on the removal of pharmaceuticals from water with micro-grain activated carbon," *Water Res.*, vol. 144, pp. 402–412, 2018, doi: 10.1016/j.watres.2018.07.037.

[32] Y. Tang *et al.*, "Upconversion particles coated with molecularly imprinted polymers as fluorescence probe for detection of clenbuterol," *Biosens. Bioelectron.*, vol. 71, pp. 44–50, Sep. 2015, doi: 10.1016/j.bios.2015.04.005.

[33] Y. Tang *et al.*, "Determination of clenbuterol in pork and potable water samples by molecularly imprinted polymer through the use of covalent imprinting method," *Food Chem.*, vol. 190, pp. 952–959, Jan. 2016, doi: 10.1016/j.foodchem.2015.06.067.

[34] T. Selkälä *et al.*, "Rapid uptake of pharmaceutical salbutamol from aqueous solutions with anionic cellulose nanofibrils: The importance of pH and colloidal stability in the interaction with ionizable pollutants," *Chem. Eng. J.*, vol. 350, pp. 378–385, Oct. 2018, doi: 10.1016/j.cej.2018.05.163.

[35] N. K. Haro, P. Del Vecchio, N. R. Marcilio, and L. A. Féris, "Removal of atenolol by adsorption – Study of kinetics and equilibrium," *J. Clean. Prod.*, vol. 154, pp. 214–219, 2017, doi: 10.1016/j.jclepro.2017.03.217.

[36] W. Xiang, Y. Zhang, H. Lin, and C. Liu, "Nanoparticle/Metal–Organic Framework Composites for Catalytic Applications: Current Status and Perspective," *Molecules*, vol. 22, no. 12, p. 2103, 2017, doi: 10.3390/molecules22122103.

[37] J. R. Li, J. Sculley, and H. C. Zhou, "Metal-organic frameworks for separations," *Chem. Rev.*, vol. 112, no. 2, pp. 869–932, 2012, doi: 10.1021/cr200190s.

[38] C. Janiak, "Engineering coordination polymers towards applications," *J. Chem. Soc. Dalt. Trans.*, vol. 3, no. 14, pp. 2781–2804, 2003, doi: 10.1039/b305705b.

[39] Y.-Y. Zhou, X.-P. Yan, K.-N. Kim, S.-W. Wang, and M.-G. Liu, "Exploration of coordination polymer as sorbent for flow injection solid-phase extraction on-line coupled with high-performance liquid chromatography for determination of polycyclic aromatic hydrocarbons in environmental materials," *J. Chromatogr. A*, vol. 1116, no. 1–2, pp. 172–178, May 2006, doi: 10.1016/j.chroma.2006.03.061.

[40] H. A. Isiyaka, K. Jumbri, N. S. Sambudi, Z. U. Zango, B. Saad, and A. Mustapha, "Removal of 4-chloro-2-methylphenoxyacetic acid from water by MIL-101(Cr) metal-organic framework: kinetics, isotherms and statistical models," *R. Soc. Open Sci.*, vol. 8, no. 1, p. 201553, Jan. 2021, doi: 10.1098/rsos.201553.

[41] J. Juan-alcan *et al.*, "Towards acid MOFs – catalytic performance of sulfonic acid functionalized architectures†," *Catal. Sci. Technol.*, vol. 101, no. Mil, pp. 2311–2318, 2013, doi: 10.1039/c3cy00272a.

[42] H. Yang *et al.*, "Determination and removal of clenbuterol with a stable fluorescent zirconium(IV)-based metal organic framework," *Microchim. Acta*, vol. 186, no. 7, p. 454, Jul. 2019, doi: 10.1007/s00604-019-3586-3.

[43] Y. Zhao *et al.*, "Metal organic frameworks for energy storage and conversion," *Energy Storage Mater.*, vol. 2, no. November, pp. 35–62, 2016, doi: 10.1016/j.ensm.2015.11.005.

[44] M. A. Chowdhury, "Metal-organic-frameworks for biomedical applications in drug delivery, and as MRI contrast agents," *J. Biomed. Mater. Res. - Part A*, vol. 105, no. 4, pp. 1184–1194, 2017, doi: 10.1002/jbm.a.35995.

[45] R. Dai, X. Wang, C. Y. Tang, and Z. Wang, "Dually Charged MOF-Based Thin-Film Nanocomposite Nanofiltration Membrane for Enhanced Removal of Charged Pharmaceutically Active Compounds," *Environ. Sci. Technol.*, vol. 54, no. 12, pp. 7619–7628, 2020, doi: 10.1021/acs.est.0c00832.

[46] J. Lv *et al.*, "Effective Removal of Clenbuterol and Ractopamine from Water with a Stable Al(III)-Based Metal-Organic Framework," *Inorg. Chem.*, vol. 60, no. 3, pp. 1814–1822, 2021, doi: 10.1021/acs.inorgchem.0c03296.

[47] M. H. Zeng, B. Wang, X. Y. Wang, W. X. Zhang, X. M. Chen, and S. Gao, "Chiral magnetic metal-organic frameworks of dimetal subunits: Magnetism tuning by mixed-metal compositions of the solid solutions," *Inorg. Chem.*, vol. 45, no. 18, pp. 7069–7076, 2006, doi: 10.1021/ic060520g.

[48] I. Ahmed and S. H. Jhung, "Composites of metal-organic frameworks: Preparation and application in adsorption," *Mater. Today*, vol. 17, no. 3, pp. 136–146, 2014, doi: 10.1016/j.mattod.2014.03.002.

[49] M. Bellusci *et al.*, "Magnetic Metal-Organic Framework Composite by Fast and Facile Mechanochemical Process," *Inorg. Chem.*, vol. 57, no. 4, pp. 1806–1814, 2018, doi: 10.1021/acs.inorgchem.7b02697.

[50] M. Bellusci *et al.*, "Manganese iron oxide superparamagnetic powder by mechanochemical processing. Nanoparticles functionalization and dispersion in a nanofluid," *J. Nanoparticle Res.*, vol. 14, no. 6, 2012, doi: 10.1007/s11051-012-0904-7.

[51] O. E. Fayemi, S. E. Elugoke, O. Dina, M. Mwanza, and P. O. Fayemi, "Harnessing Fe3O4 Screen-Printed Modified Electrode Sensor for Detecting Epinephrine in Buff Orpington Rooster and Rhodes Island White Broiler," *Front. Sensors*, vol. 3, Mar. 2022, doi: 10.3389/fsens.2022.850316.

[52] N. R. Jannah and D. Onggo, "Synthesis of Fe3O4 nanoparticles for colour removal of printing ink solution," in *Journal of Physics: Conference Series*, Oct. 2019, vol. 1245, no. 1. doi: 10.1088/1742-6596/1245/1/012040.

[53] L. Li, X. L. Liu, H. Y. Geng, B. Hu, G. W. Song, and Z. S. Xu, "A MOF/graphite oxide hybrid (MOF: HKUST-1) material for the adsorption of methylene blue from aqueous solution," *J. Mater. Chem. A*, vol. 1, no. 35, pp. 10292–10299, 2013, doi: 10.1039/c3ta11478c.

[54] M. Anbia and V. Hoseini, "Development of MWCNT@MIL-101 hybrid composite with enhanced adsorption capacity for carbon dioxide," *Chem. Eng. J.*, vol. 191, pp. 326–330, 2012, doi: 10.1016/j.cej.2012.03.025.

[55] I. Ahmed and S. H. Jhung, "Applications of metal-organic frameworks in adsorption/separation processes via hydrogen bonding interactions," *Chem. Eng. J.*, vol. 310, pp. 197–215, 2017, doi: 10.1016/j.cej.2016.10.115.

[56] Z. U. Zango *et al.*, "A Critical Review on Metal-Organic Frameworks and Their Composites as Advanced Materials for Adsorption and Photocatalytic Degradation of Emerging Organic Pollutants from Wastewater," *Polymers (Basel).*, vol. 12, no. 11, p. 2648, Nov. 2020, doi: 10.3390/polym12112648.

[57] N. Stock and S. Biswas, "Synthesis of Metal-Organic Frameworks (MOFs): Routes to Various MOF Topologies, Morphologies, and Composites," *Chem. Rev.*, vol. 112, no. 2, pp. 933–969, Feb. 2012, doi: 10.1021/cr200304e.

[58] Z. U. Zango, K. Jumbri, H. F. M. Zaid, N. S. Sambudi, and J. Matmin, "Optimizations and artificial neural network validation studies for naphthalene and phenanthrene adsorption onto NH2-UiO-66(Zr) metal-organic framework," *IOP Conf. Ser. Earth Environ. Sci.*, vol. 842, no. 1, 2021, doi: 10.1088/1755-1315/842/1/012015.

[59] A. Mahmad, M. S. Shaharun, Z. U. Zango, T. U. Noh, and B. Saad, "Adsorptive Removal of Bisphenol A Using Zeolitic Imidazolate Framework (ZIF-8)," *Springer Proc. Complex.*, pp. 117–129, 2021, doi: 10.1007/978-981-16-4513-6_11.

[60] A. Mahmad, M. Shima Shaharun, T. Ubaidah Noh, Z. Uba Zango, and M. Faisal Taha, "Experimental and molecular modelling approach for rapid adsorption of Bisphenol A using Zr and Fe based metal–organic frameworks," *Inorg. Chem. Commun.*, vol. 142, no. March, 2022, doi: 10.1016/j.inoche.2022.109604.

[61] Saruchi and V. Kumar, "Adsorption kinetics and isotherms for the removal of rhodamine B dye and Pb +2 ions from aqueous solutions by a hybrid ion-exchanger," *Arab. J. Chem.*, vol. 12, no. 3, pp. 316–329, 2019, doi: 10.1016/j.arabjc.2016.11.009.

[62] A. C. Tella, S. O. Owalude, C. A. Ojekanmi, and O. S. Oluwafemi, "Synthesis of copper-isonicotinate metal-organic frameworks simply by mixing solid reactants and investigation of their adsorptive properties for the removal of the fluorescein dye," *New J. Chem.*, vol. 38, no. 9, pp. 4494–4500, 2014, doi: 10.1039/c4nj00411f.

[63] K. Nakamoto, "Infrared and Raman Spectra of Inorganic and Coordination Compounds," *Handb. Vib. Spectrosc.*, pp. 1872–1892, 2006, doi: 10.1002/9780470027325.s4104.

[64] L. Nalbandian, O. Mahmoud, and H. A. Nasr-El-Din, "New Magnetite Nanoparticles Allow Smart Drilling Fluids with Superior Properties CO2 foam for Hydraulic fracturing and EOR applications View project Manganese Tetraoxide-based drilling fluids View project," 2017. [Online]. Available: https://www.researchgate.net/publication/322163633

[65] S. Zavareh, Z. Behrouzi, and A. Avanes, "Cu (II) binded chitosan/Fe3O4 nanocomomposite as a new biosorbent for efficient and selective removal of phosphate," *Int. J. Biol. Macromol.*, vol. 101, pp. 40–50, Aug. 2017, doi: 10.1016/j.ijbiomac.2017.03.074.

[66] Y. H. Liu, Y. L. Lu, H. L. Tsai, J. C. Wang, and K. L. Lu, "Hydrothermal synthesis, crystal structure, and magnetic property of copper(II) coordination networks with chessboard tunnels," *J. Solid State Chem.*, vol. 158, no. 2, pp. 315–319, 2001, doi: 10.1006/jssc.2001.9118.

[67] A. Pichon, A. Lazuen-Garay, and S. L. James, "Solvent-free synthesis of a microporous metal-organic framework," *CrystEngComm*, vol. 8, no. 3, pp. 211–214, 2006, doi: 10.1039/b513750k.

[68] M. Rabiei, A. Palevicius, A. Monshi, S. Nasiri, A. Vilkauskas, and G. Janusas, "Comparing methods for calculating nano crystal size of natural hydroxyapatite using X-ray diffraction," *Nanomaterials*, vol. 10, no. 9, pp. 1–21, 2020, doi: 10.3390/nano10091627.

[69] H. Unterweger *et al.*, "Hypericin-bearing magnetic iron oxide nanoparticles for selective drug delivery in photodynamic therapy," *Int. J. Nanomedicine*, vol. 10, pp. 6985–6996, Nov. 2015, doi: 10.2147/IJN.S92336.

[70] S. Duan and Y. Huang, "Electrochemical sensor using NH2-MIL-88(Fe)-rGO composite for trace Cd2+, Pb2+, and Cu2+ detection," *J. Electroanal. Chem.*, vol. 88, no. October, 2017, doi: doi.org/10.1016/j.jelechem.2017.11.051.

[71] H. Shagholani, S. M. Ghoreishi, and M. Mousazadeh, "Improvement of interaction between PVA and chitosan via magnetite nanoparticles for drug delivery application," *Int. J. Biol. Macromol.*, vol. 78, no. November 2017, pp. 130–136, 2015, doi: 10.1016/j.ijbiomac.2015.02.042.

[72] Y. Chen, L. Li, J. Li, K. Ouyang, and J. Yang, "Ammonia capture and flexible transformation of M-2(INA) (M=Cu, Co, Ni, Cd) series materials," *J. Hazard. Mater.*, vol. 306, pp. 340–347, 2016, doi: 10.1016/j.jhazmat.2015.12.046.

[73] G. Shi, W. Xu, J. Wang, Y. Yuan, S. Chaemchuen, and F. Verpoort, "A Cu-based MOF for the effective carboxylation of terminal alkynes with CO2under mild conditions," *J. CO2 Util.*, vol. 39, no. May, p. 101177, 2020, doi: 10.1016/j.jcou.2020.101177.

[74] A. A. Aryee *et al.*, "Selective removal of anionic dyes in single and binary system using Zirconium and iminodiacetic acid modified magnetic peanut husk," *Environ. Sci. Pollut. Res.*, no. 100, Mar. 2021, doi: 10.1007/s11356-021-13030-5.

[75] V. Vadivelan and K. V. Kumar, "Equilibrium, kinetics, mechanism, and process design for the sorption of methylene blue onto rice husk," *J. Colloid Interface Sci.*, vol. 286, no. 1, pp. 90–100, Jun. 2005, doi: 10.1016/j.jcis.2005.01.007.

[76] P. Waranusantigul, P. Pokethitiyook, M. Kruatrachue, and E. S. Upatham, "Kinetics of basic dye (methylene blue) biosorption by giant duckweed (Spirodela polyrrhiza)," *Environ. Pollut.*, vol. 125, no. 3, pp. 385–392, Oct. 2003, doi: 10.1016/S0269-7491(03)00107-6.

[77] H. A. Isiyaka, K. Jumbri, N. S. Sambudi, Z. U. Zango, N. A. F. B. Abdullah, and B. Saad, "Optimizations and docking simulation study for metolachlor adsorption from water onto MIL-101(Cr) metal–organic framework," *Int. J. Environ. Sci. Technol.*, vol. 101, no. 0123456789, 2022, doi: 10.1007/s13762-022-04059-1.

[78] Z. U. Zango *et al.*, "Adsorption of chrysene in aqueous solution onto MIL-88(Fe) and NH2-MIL-88(Fe) metal-organic frameworks: Kinetics, isotherms, thermodynamics and docking simulation studies," *J. Environ. Chem. Eng.*, vol. 8, no. 2, p. 103544, Apr. 2020, doi: 10.1016/j.jece.2019.103544.

 doi:10.20944/preprints202212.0434.v1

[79] A. Tella, F. Nwosu, and V. Adimula, "Removal of Anthracene from solution using [Cu(INA)2] metal- organic frameworks synthesized by a solvent free method.," *Niger. J. Mater. Sci. Eng.*, vol. 7, p. 26, 2016.